University of California

Ernest O. Lawrence Radiation Laboratory

Berkeley, California

DISCLAIMER

Being revised for journal publication UCRL-10606

UNIVERSITY OF CALIFORNIA
Lawrence Radiation Laboratory
Berkeley, California

Contract No. W-7405-eng-48

QUENCH HARDENING IN COPPER

James Martin Galligan

Thesis

January 1963

Table of Contents

Quench Hardening In Copper

Degree: Doctor of Philosophy J.M. Galligan Major Subject: Metallurgy

_____(Chairman)
Thesis Committee

The removal of excess vacancies in quenched single crystals of copper has been studied by three techniques: electrical resistivity, small angle scattering of X-rays and tensile deformation. These results indicate that small clusters of vacancies or isolated vacancies do not harden quenched crystals, but larger clusters, obtained by aging, drastically change the mechanical properties.

The observed change in yield stress is consistent with a model of hardening proposed by Coulomb and Friedel, which suggests that the breakaway of dislocations from vacancy clusters determines the yield stress. The observed temperature dependence of the yield stress is also consistent with this model. Also, the observed change in work hardening in quenched and aged specimens is explained by assuming that gliding dislocations when interacting with vacancy clusters allow subsequent movement of other dislocations on the same plane would then be somewhat easier. As a result of this action, there would be fewer and fewer obstacles to the motion of dislocation. This would tend to favor isolated, thick slip bands and could decrease the interaction between gliding dislocations on non-parallel slip bands.

Introduction:

A detailed understanding of the strain hardening of a metal crystal, as evidenced by its macroscopic stress-strain behavior, in terms of the microscopic distribution, motion and interaction of dislocations represents one of the major unresolved problems in physical metallurgy.* A treatment of the strain hardening which accompanies plastic deformation of crystals not only involves dislocations but also point defects since it is believed that non-equilibrium concentrations of point defects are also introduced by plastic deformation.(1) However, because more than one species of defect is introduced simultaneously during deformation, it is difficult to assess the relative hardening which results from the various interactions between the different types of defects involved. Thus, Hirsch(2) and Mott(3) have proposed that the major cause of hardening in stage II of face-centered cubic metals is due to the formation of sessile jogs as a result of the intersection of dislocations. Another interpretation of the strain hardening behavior which considers that the jogs are formed during the strain hardening process by the interaction of point defects with dislocations, has been given by Kuhlmann-Wilsdorf.(4) This theory, in particular, relates the major part of

---

* See the recent review by Hargreaves and Clarebrough, Progress in Metal Physics, Vol. 7 (1959), 81.

strain hardening to dislocation-vacancy interactions.

Since quenching a metal retains a large excess of vacancies,[5] its stress-strain behavior might be significantly altered if the quenched-in vacancies are annihilated at dislocations, and attempts have been made to study this effect by observing the stress-strain behavior of quenched crystals. Li, Washburn and Parker[6] rapidly cooled large single crystals of zinc and then deformed them in pure shear. They found a small but reproducible increase in yield stress-about 20% higher than in furnace cooled crystals-but no substantial change in the shape of the stress-strain curve.

Another sink for the excess vacancies retained by quenching was first discussed by Seitz[7] as a means of explaining the dislocation networks observed in metal crystals. He proposed that the excess vacancies retained by quenching could migrate at relatively low temperatures and agglomerate to form platelike voids, which could then collapse to form dislocation loops. These predictions were strikingly confirmed by Hirsch et al,[8] in an examination of quenched aluminum crystals using transmission electron microscopy. Hirsch and co-workers also observed other related phenomena such as large jogs on the randomly oriented dislocations initially present, and stacking fault tetrahedra in quenched

and aged gold specimens.

In general three types of defects have been observed in quenched and aged metals, namely, Frank sessile dislocations, prismatic dislocation loops and stacking fault tetrahedra. In a face-centered cubic metal, the collapse of a disc of vacancies on a (111) results in the formation of a stacking fault bounded by a partial dislocation (Frank) with a Burgers vector 1/3 [111] . If the stacking fault energy of the metal is very high, it is energetically favorable to nucleate a Shockley partial to remove the fault and to combine with the Frank partial. In metals of intermediate stacking fault energy, loops are expected to be Frank partials enclosing stacking faults. However, the Frank sessile dislocation has a relatively large Burgers vector and the associated energy can be reduced at the expense of creating more stacking fault by a dissociation into stair-rod dislocations. This reaction is the basis of the observed stacking fault tetrahedra in quenched gold. In general, then, the stable type of defect depends on the stacking fault energy of the metal. All three types of defects have been observed by transmission electron microscopy.

Evidence of quench hardening has been given by Maddin and Cottrell,[9] who observed a marked increase of yield stress in

quenched aluminum crystals - an order of magnitude increase - as well as a stage following yielding in which strain hardening was small. These authors also showed that quenched aluminum crystals exhibit coarse surface slip lines whereas slowly cooled specimens normally show only fine slip. Other observations[9] have shown not only a change in surface slip pattern but also a change in deformation texture, as well as overshooting of the symmetry orientation, similar to that observed in the deformation of alpha-brass crystals. A large decrease in the internal friction has also been observed in quenched and aged aluminum crystals,[10] which was attributed to the pinning of dislocations by excess vacancies.

More recently Meshii and Kaufman[11] and Kimura, Maddin and Kuhlmann-Wilsdorf[12] have studied quench hardening in polycrystalline gold and copper, respectively. Their results agree to a large extent, especially for specimens quenched from the highest temperatures. The general shape of the stress-strain curves observed by Meshii and Kaufman for freshly quenched and for quenched and aged specimens was substantially the same as that of slowly cooled specimens, except for the increase in stress. Kimura, Maddin and Kuhlmann-Wilsdorf did not determine the entire stress-strain curve and hence no detailed comparison can be made.

In order to interpret these rather diverse observations, many suggestions have been made.[11][12][13] These have generally centered around three mechanisms of strain hardening which will be outlined below. Point defects, whether they are clustered or not, can attach themselves to dislocations and thereby form jogs. Recently, Hirsch[2] has emphasized that jogs in split dislocations can be sessile and, therefore, can lead to a hardening. Much the same viewpoint has been expressed by Cottrell[1] and by Coulomb and Friedel.[14] However, these interpretations are somewhat different in that Cottrell considers the vacancies to be annihilated forming jog pairs once they reach the dislocation, whereas Coulomb and Friedel suggest that vacancies, upon reaching a dislocation, will diffuse along it, and in so doing meet other vacancies, eventually agglomerating to form voids along the dislocation. A second possibility is that a dispersion of isolated point defects, or perhaps small clusters of point defects, can give rise to a hardening due to their interaction with moving dislocations. Finally, it has been suggested that the major source of hardening is not due to isolated vacancies but rather to the final product of the clustering, namely, dislocation loops or stacking fault tetrahedra.[15] Here again there are different proposals on just how loops or tetrahedra, can give rise to a large increase in yield stress. Kuhlmann-Wilsdorf[15] originally suggested that loops could

originally suggested that loops could act as small Frank-Read sources. Kroupa,[16] and Saada and Washburn[17] have recently considered the interaction of a glissile dislocation with a dislocation loop and find that both long-range and short-range interactions are possible.

While all of the mechanisms briefly outlined above give reasonable values for the hardening observed in quenched crystals, not one is completely satisfactory. For instance, in the jog hardening theories, estimates are made of the constriction energies of jogs using linear elasticity theory in the very range in which it is not expected to apply. Another criticism is the lack of consideration, in the various intersection mechanisms, of the velocities of the mobile dislocations involved. For instance, Weertman[18] has recently shown that dislocations of like sign can attract in certain velocity ranges, whereas under static conditions they normally repel. In some velocity regions, then, no interaction will occur. A somewhat similar situation could conceivably apply to the interactions of vacancies and moving dislocations.

The experiments have not allowed clear cut distinctions to be made, in favor of any of the various mechanisms and so have only really shown that there is a hardening associated with quenching. Also, the processes that have been considered must overlap. Thus, while clusters of vacancies

are forming after quenching, vacancies are also diffusing to dislocations. This is especially true during the initial stages of the aging process, while in the intermediate stages, clusters can be collapsing to form dislocation loops or stacking fault tetrahedra. In the final stages, prior to aging in a temperature range where the remaining clusters of vacancies or loops might be expected to disappear, further shrinkage of voids can be expected. Thus, one might expect a decrease in cluster size with time and a growth of dislocation loops. Simultaneously the mean length and density of dislocation jogs can be changing.

In order to understand more fully the nature of quench hardening and its relation to strain hardening the following experiments were undertaken: A large supersaturation of vacancies was introduced into single crystals of copper by quenching from high temperatures and the subsequent annihilation of the excess vacancies was studied using three techniques - electrical resistivity, small angle scattering of x-rays and tensile deformation. Briefly, the first of these techniques measures the removal of the supersaturation of single vacancies, divacancies, or trivacancies, whereas the second measures the accumulation of vacancies as voids or clusters, but does not measure their disappearance at dislocations. It was expected that by correlating the results

of these measurements with the stress-strain behavior after various quenching and aging treatments, the role which point defects play in strain hardening might be further clarified.

Experimental Procedure

Specimen material for these experiments was 99.999% pure copper obtained from two sources: The copper used in the small-angle scattering experiments was obtained from American Smelting and Refining Company and was specified to be spectroscopically pure. That used in the resistivity and mechanical tests was also American Smelting and Refining Company spectroscopically pure copper which was drawn into wire by Sigmund Cohn Co., Mount Vernon, N.Y.

A. Small Angle Scattering Techniques

Flat single crystals of copper were grown by the strain anneal method by reducing the thickness of copper bars by more than 95%. Specimens were subsequently heated in an evacuated mullite tube (pressure $< 10^{-5}$ mm. Hg.) for about 30 minutes at 600°C followed by four days at 1030°C. This resulted in relatively perfect crystals.

X-Ray Technique

The x-ray generator was a Hilger fine focus x-ray unit, employing a Cu target. The unit was generally operated at 40KV and 2 ma. An asymmetrical curved crystal of quartz was used in conjunction with this x-ray generator. A schematic drawing, Fig. 1, illustrates the geometry used throughout these experiments. The source slit used limited the divergence of the beam to less than ½ degree; the detector slit had a width of less than one thousandth of an inch, or approximately $\frac{1}{3} \times 10^{-4}$ radians in subtended arc. With the use of a helium tunnel, intensities in the range from 2×10^{7} to $\frac{1}{3} \times 10^{6}$ cps were obtained. Sample temperatures throughout were maintained at 78°K except when the temperature dependence of the scattering was measured. The helium used in the helium tunnel was passed through a copper coil immersed in liquid nitrogen to remove any traces of water. During the elapsed time of measurement, about ½ hours, no ice was observed to form on the specimen. All scattering curves were corrected for parasitic scattering. Corrections for slit height were calculated and found to be negligible in the angular range of the experiments.

The scattering of x-rays at small angles arises from local in-

homogeneities in a solid.[19] When these inhomogeneities are of the same order of magnitude as the wavelength of the impinging x-ray beam, their disturbance of the periodicity of the crystal lattice leads to scattering of x-rays. The angle through which the x-rays are scattered at very small angles, i.e. from $\frac{1}{4}$ to $\frac{1}{2}^{\circ}$, depends only upon the size of the inhomogeneities causing the scattering. But at higher angles, e.g., in the range from $\frac{1}{2}$ to 3°, the scattered intensity at any angle is determined by the shape as well as the size of the scattering center. Unfortunately, however, the difference in the scattered intensity caused by particles of different shape is usually not sufficient to allow clear cut distinctions to be made. The scattered intensity from spheres, and circular discs of infinitesimal height have been drawn in Fig. 2. These figures show that particles of very different shapes can have nearly the same scattering curves. Another bad feature of the results obtained by small angle scattering of x-rays is the following: The intensity received at any angle is very largely determined by the largest particles, since the scattered intensity for any given angle of scattering depends upon the sixth power of the radius of gyration of the scattering center involved. Thus, without some idea of the distribution of sizes involved in a scattering experiment, the size

measured cannot be taken as the average but must be nearer the maximum size present.

Quenching Procedure

Quenching must be sufficiently rapid to retain a sizeable fraction of the vacancies and yet be conducted so as to avoid appreciable quenching deformation. Specimens were suspended within a cage fabricated from Cu wire inside an induction coil so that they were approximately $\frac{1}{2}$ inch above a calcium chloride-water quenching bath (bath temperature: - 20°C). The bath was large in mass so that the temperature remained approximately constant when the specimen was dropped. Furthermore, the path length of the specimen in the bath was long, so that any bubbles would be brushed away by continued motion of the specimen. The temperature from which the specimen was quenched was measured with an optical pyrometer; corrections were made for the emissivity of the Cu and the absorption of the glass. The estimated average quenching rate obtained with this arrangement was 10^4 deg./sec. which is comparable to that used by Bauerle and Koehler[5] in quenching experiments with Au. A very rough estimate of the excess concentration of vacancies obtained by this quenching method, using the

energy of formation of vacancies in Cu as 1.1 e.v., gives about 1×10^{-3}.

Preliminary experiments using a tubular furnace and a larger distance between the hot zone and the quenching bath did not produce satisfactory results. This is shown by the initial small angle scattering obtained with the slow and fast quenches, Fig. 3.

B. Electrical Resistivity

A standard four lead resistor method was used to measure electrical resistivity. The current was monitored by measuring the potential drop across a calibrated 1ohm Manganin resistor in series with the test specimen. The Manganin resistor was so-called 29% Manganin wire with a temperature coefficient of less than 1 part in 10^5 per degree. This resistor was baked at 200°C for two days prior to calibration so that no long term drifts would be expected at room temperature. The current source was a d.c. current supply, which was previously described by Garwin,[20] and maintained the current constant to within 1 part in 10^5. The potential developed with one tenth amp was measured with a Rubicon Thermofree potentiometer, model 2768, which could detect 1/100 of a microvolt. All resistance measurements were made at 78°K by immersing the specimen in a stirred liquid nit-

rogen bath.

It should also be mentioned that many unsuccessful attempts were made to spot weld copper potential leads to the test section of the specimen but no reproducible method was found. The final method which was found to be satisfactory was to sinter the leads to the copper specimens by heating the specimen assembly to approximately 900°C. This method also avoided the contamination and plastic deformation that might result from spot welding.

C. Crystal Growth

Crystals, all of the same orientation, 0.016 in. in diameter were grown by a soft mold technique in a tubular furnace. Ten to twelve specimens were grown simultaneously from a flat seed in a grooved graphite mold. The uniformity of cross-section of the crystals obtained by this technique was very good.

D. Annealing and Quenching Procedures of Copper Wires

The single crystal wires were suspended horizontally between two copper electrodes spaced approximately 5 inches apart. The specimens were passed through a hole in the electrodes and were

held in place by tightly packing graphite powder in the hole. The graphite powder served both as a good electrical contact and it also allowed the specimen to expand freely. Specimens were heated electrically in a purified atmosphere of helium. No oxidation of the specimens was observed, the surfaces remaining bright after more than five hours at temperature. Prior to annealing the specimens were chemically polished, rinsed in distilled water and washed in absolute alcohol. In specimens quenched from approximately 1070°C and aged very short times at room temperature no hardening was observed, so that any deformation introduced by this quenching technique must be small.

The quenching procedure itself consisted insimultaneously admitting precooled helium gas into the chamber and cutting the power input to the specimen with a double-pole, double-throw relay. This relay simultaneously opened a valve to admit the helium quench gas and simultaneously cut the current to zero. Temperatures were measured using an optical pyrometer, corrections being made for the emissivity of the copper and for absorption in the sight glass.

2. Tensile Tests

For the determination of stress-strain curves a tensile

machine was constructed, Fig. 4. The drive for the machine was provided by the chart motor of a Speedomax recorder. The load-extension curve was also displayed on the recorder. The load sensing element of the machine was a linear differential transformer, which was placed at the center of a circular ring (proving ring) in series with the specimen. The load sensing device was calibrated directly by dead loading with measured loads. The signal from the load coil was found to vary linearly in the range of loads used in all subsequent tests. All tensile tests, except for the temperature dependence of the yield stress, were conducted at 78°K, using a helium exchange gas as a transfer medium between the walls of the gas cap and the specimen.

The self-aligning specimen grips were of the standard split type with an axial groove at their centers, which insured firm clamping of the specimen throughout the test. The measured total extension after deformation was found to agree quite well with the extension measured on the chart of the Speedomax recorder. When fracture occurred it was always within the gauge length. In order to eliminate any possible preloading due to differences of thermal contraction between the gripping assembly and the specimen, such as might arise when cooling the specimen to lower temperatures,

the pinhole in the lower (stationary) grip was made somewhat larger than the tapered pin used to attach the lower grip to the fixed frame of the machine. The pin itself fitted into a matching tapered hole in the bottom frame of the tensile machine. When this tapered pin was placed firmly in position, no preloading of the specimen occurred when temperature changes were made.

The initial strain rate used throughout these measurements was approximately 10^{-4}/sec. To measure the temperature dependence of the yield stress of the quenched specimens at 4.2°K, the gas cap was surrounded by a double glass dewar, the inner dewar filled with liquid helium and the outer one with liquid nitrogen. Other temperatures were attained using various fixed temperature baths surrounding the gas cap.

Presentation of Results and Discussion

A. Small-Angle Scattering From Quenched Specimens

The radius of gyration observed in samples quenched from high temperatures, as well as its variation with subsequent aging, are shown in Fig. 3. This radius of gyration is obtained in the following manner. It is well known that the intensity scattered as a function of angle is proportional to the square of structure factor.[19]

$$I(\varepsilon) = K F^2(\varepsilon)$$

where I is the intensity scattered at angle ε, F the structure factor, and K a constant of proportionality. Guinier has shown that the structure factor can be approximated by an exponential function,

$$F^2 = F^2(0)\, e^{-\varepsilon^2 R_0^2}$$

where R_0 is the radius of gyration of the particle causing the scattering, which has an electron density different from the surrounding matrix. This expression can be written as

$$\log F^2 = -\frac{\varepsilon^2 R_0^2}{3} \log e + \text{Const.}$$

from which we obtain an expression for the scattered intensity as a function of angle,

$$\log I = -\frac{\varepsilon^2 R_0^2}{3} \log e + \text{Const.}$$

The method of analysis is thus simple: The logarithm of the experimentally determined intensity is plotted versus ε^2 and from this plot a slope is obtained. This slope is directly proportion-

al to the square of the radius of gyration of the scattering center.

Consider first the scattering observed at 78°A, in copper quenched from 1060°C at "zero" time. This scattering is, within experimental error, zero at "zero" time, Fig. 5. This indicates that a) clusters of excess vacancies retained by quenching must be smaller than 10Å. b) no appreciable ~~do~~ Bragg scattering has been introduced by any deformation which might have occurred in the quenching procedure. c) the finite slope at zero aging time, on the other hand, indicates that clusters of vacancies are indeed present immediately after quenching. Shown in Fig. 6 are the results of a slower quenching procedure. While the shape of the scattering curves were similar for "slow" and "fast" quenches, the results definitely indicate that some larger clusters might initially be present after the slower quench.

The gradual increase of the size of clusters, in a quenched specimen, with time can be given the following interpretation: Single excess vacancies and the smallest clusters continuously disappear as vacancies are absorbed by the larger clusters.

Theoretical calculations of the scattered intensity as a function of scattering angle have been made for particles of

various shapes. Rayleigh[21] showed that the scattering for spheres should be given by

$$I(\varepsilon) = \left[\frac{3\sin\varepsilon R_0 - \varepsilon R_0 \cos\varepsilon R_0}{\varepsilon^3 R_0^3}\right]$$

Kratky and Porod[22] have calculated the intensity scattered as a function of scattering angle for discs of radius R and infinitesimal height and found

$$I(\varepsilon) = \frac{2}{\varepsilon^2 R_0^2}\left[1 - \frac{J_1(2\varepsilon R_0)}{\varepsilon R^0}\right]$$

where $J_1(2\varepsilon R_0)$ is a Bessel function of order 1. A comparison of the observed intensity was made with the tabulated values given by Guinier et al.[19] for the above expressions. These theoretical curves allowed comparison of the experimental results with the scattering expected for particles of various shapes. This comparison is shown in Fig. 11. From this comparison it can definitely be seen that the experimental results more closely resemble the theoretical scattering curve for spheres than for platelets of infinitesimal height. The theoretical relations are, however, not precise enough, nor is the experimental data of sufficient accuracy, to rule out the possibility that the clusters might have a flat, ellipsoidal shape.

The number of vacancies associated with a sphere of the same

size as the maximum radius observed in these experiments would be approximately 3000. If we consider the scattering centers to be ellipsoids, the total volume and thus the number of vacancies in these clusters would be much smaller. Some estimates have been made of the minimum number of vacancies which if clustered might collapse to form a dislocation loop or stacking fault tetrahedron. Silcox and Hirsch[23] have given this number as 7400 for the tetrahedra they have observed in quenched and aged gold. Wilsdorf and Kuhlmann-Wilsdorf[24] have given rough estimates of the number of excess vacancies which must agglomerate in a quenched metal in order to have nucleation of dislocation loops occur. They obtain anywhere from 80 to 200 vacancies as the number of vacancies which must agglomerate for nucleation to occur.

After aging two years at room temperature, the quenched and aged copper specimen was examined in transmission electron microscopy in a Siemens electron microscope. While small black spots were observed, no clearly defined dislocation loops were present, Figs. 7, 8. Similar observations have been made in quenched gold when aged at room temperature, Fig. 9, 10. Since no dislocation loops were observed in quenched and aged copper as well as similar-

ly treated gold, one can look to the difference in aging temperature used here compared with that used by Silcox and Hirsch. Aging at 120°C for Cu[25] and at 100°C for gold[23] was necessary to produce dislocation loops and tetrahedra. This treatment could lead to very different nucleation and growth conditions than that used in the present experiments. The growth rates would be two or three orders of magnitude greater. In the present experiments the size which was attained by the dislocation loops or clusters during the low temperature aging was apparently large enough to be resolved by the electron microscope.

To further demonstrate that the small angle scattering observed in quenched and aged specimens was not due to double Bragg scattering the temperature dependence of scattered intensity was measured. The temperature dependence of the scattering of x-rays at small angles should increase with increasing temperature if the scattering arises from true small-angle scattering.[26] If the scattering arises from double-Bragg scattering the intensity should decrease with increasing temperature. The small angle scattering was measured, at a fixed scattering angle, as a function of temperature for a fully aged specimen which had been quenched from

1060°C. These results are shown in Fig. 12. They clearly demonstrate that the observed scattering cannot be related to double-Bragg scattering.

B. Electrical Resistivity Measurements

Single crystal wires were quenched from approximately 1060°C and the decay of the excess quenched-in resistivity was measured at 78°K after aging for various times at room temperature. When sufficient precaution was taken to avoid large plastic deformation in the measuring procedure, the quenched-in resistivity was found to decay monotonically with aging time at room temperature. These results are shown in Fig. 13. In specimens that were deformed during the measuring procedure, the results were not reproducible, Fig. 14. No explanation for this behavior will be given here.

The results are similar to those obtained by Seeger, et. al.[27] There was a spread of about 2 in the total change of resistivity for specimens quenched from the same temperature. The total decay time for the removal of the excess resistivity observed in these experiments was about 150 minutes in specimens quenched from 1060°C

and aged at 25°C. The removal of this excess resistivity in about 2½ hours presumably corresponded to the annihilation of excess vacancies at various sinks. These sinks could be clusters of vacancies, surfaces and dislocations. The resistivity measurements do not distinguish between the various kinds of sinks. Also, if there was competitive growth of clusters, with smaller clusters disappearing and larger ones growing, resistivity measurements would probably not be sensitive to such changes. Resistivity, as mentioned in the introduction, measures largely the removal of the excess isolated vacancies or mobile divacancies from the lattice.

C. Tensile Tests

The stress-strain curves obtained at 78°K for crystals oriented for single slip and for multiple slip are shown in Figs. 15 through 30. For comparison purposes, the corresponding curves for unquenched crystals are also given in these figures. Prior to quenching each sample, a length of about two inches was cut from one end; these unquenched crystals were also tested at 78°K. This served the two-fold purpose of providing both a blank and a gauge

of the extent of hardening in the quenched portion of the same specimen. This procedure tends to reduce uncontrollable variations in purity and dislocation structure from specimen to specimen. The stress-strain curves for quenched and unquenched samples could then be compared directly at each stage of the aging process. It is convenient to consider separately the stress-strain behavior corresponding to the initial, the intermediate and the final stages of aging of quenched specimens at room temperature.

i) Initial Stages of Aging in Quenched Crystals - Times Less Than Ten Minutes

The stress-strain behavior for quenched specimens aged less than ten minutes at room temperature was indistinguishable from that for unquenched specimens, within the spread noticed in these experiments. This applies both to crystals oriented for single slip and to those oriented for multiple slip. These curves are shown in Figs. 15, 23, 24. Three rather definite conclusions may be drawn from these results: a) the deformation introduced by the quenching procedure was negligible. b) the yield stress in

quenched crystals was not greatly influenced by excess vacancies which existed either as isolated defects or as small clusters. c) since the work hardening above the yield stress was substantially the same in quenched and unquenched specimens, isolated vacancies or small vacancy clusters did not greatly influence the work hardening rate.

Measurements of the small-angle scattering revealed that the maximum cluster size developed after aging about 10 minutes was less than 10Å. It seems clear, therefore, that vacancy clusters of this size or smaller do not radically alter the deformation process, as revealed by the stress-strain curve. Nevertheless, the moving dislocations must encounter small clusters of vacancies, which are more or less randomly dispersed throughout the crystal. Therefore, it can be concluded that cutting of these small clusters by dislocations must be a comparitively easy process. Also, if vacancies diffuse to existing dislocations in the short aging times involved, thereby forming jogs, those jogs apparently do not interfere with the multiplication process (i.e. they do not in-

fluence the yield stress) nor do they have an important effect upon the work hardening rate.

Consider next the temperature dependence of the yield stress for a quenched crystal oriented for single slip which had been aged approximately 10 minutes at room temperature. As shown in Fig. 32, the yield stress increases slightly in going from room temperature to 78°K and a somewhat greater increase of the yield stress occurs between 78°K and 6°K. This rise in the yield stress between 78°K and 6°K is significantly greater than in the corresponding unquenched specimen. It is to be expected that the critical temperature below which a cluster of vacancies will begin to act as an effective barrier to moving dislocations will decrease as the size of the cluster decreases. This will be considered in detail in the next section.

ii) Intermediate Stages of Aging--Ten Minutes to Ten Hours Aging Time

In crystals quenched and aged for more than ten minutes at room temperature, pronounced changes in the stress-strain curves

occurred when specimens were tested at 78°K. The data obtained are reproduced in Figs. 16-21 and 24-28. The results indicated that: a) Within the strain sensitivity of the measurements, the slopes of the stress-strain curves below the yield stress were significantly greater in the quenched and aged crystals than in the unquenched crystals. b) The yield stress increased with increasing aging time. c) Above the yield stress, the work hardening rate of crystals oriented for single slip increased rapidly with aging, while for crystals oriented for multiple glide the work hardening rate was relatively independent of the aging time.

The significance of these observations will now be discussed in turn. Consider first the decrease in the preyield plastic flow, which has been observed in the quenched and aged specimens at stresses below the macroscopic yield stress. Small angle scattering results, mentioned above, showed a growth of clusters in these times. This suggests that at a given stress the average velocity of dislocations is decreased by the presence of clusters.

A model has been developed by Coloumb and Friedel[14] in order to account for the hardening observed in radiation damaged

materials. This model may also be applicable to quenched and aged specimens and it will therefore be considered in detail below.

The model is based on an analysis of the interaction which occurs when mobile dislocations cut through clusters of vacancies. Colomb and Friedel assumed that if there is to be hardening from cavities, the average distance between cavities, l, must be smaller than the distance at which multiplication of dislocations occurs by the operation of Frank-Read sources. It is also assumed that the force pinning the dislocation to the cluster is large compared to the applied stress. The dislocation is considered to break away from the cavity with the assistance of thermal activation when a sufficiently large thermal fluctuation occurs. Since a part of the elastic strain field is relaxed when a dislocation passes through a cavity, dislocations in a crystal containing randomly distributed voids will have a zig zag shape. The average distance between cavities on the line will depend on the density of cavities and the interaction energy. The sketch shows two successive positions of such a zig zag dislocation. The motion was due to escape from the

from the void at B.

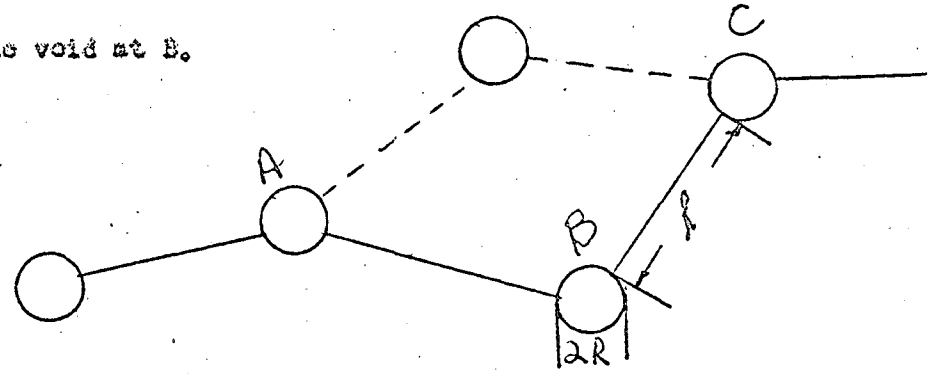

Each time the line escapes from a void it will sweep over an area about l^2 where l is the length between pinning points. The details of the escape are considered below.

Initially, under the action of the applied stress, σ, the dislocation segments AB, BC will bow out. The energy necessary to free the loops AB, BC from the cavity is the energy needed to transfer the dislocation from its equilibrium position to a position where it can break loose under the action of the applied stress. In order for this to occur, a new segment of dislocation must be formed of length approximately equal to the diameter of the cavity. Since the energy per unit length of dislocation is given approximately by $\frac{\mu b^2}{2}$ the total energy required to form the new length

of dislocation would be $\frac{\mu b^2}{2} 2R$

where R is the radius of the vacancy cluster, μ is the shear modulous and b is the Burgers vector. When the dislocation moves to the breakaway position, work is done by the applied stress; this work is proportional to the area swept out by the dislocation and is given approximately by: $\sigma b l R$

The activation energy, U, for this breakaway process will then be given by

$$U = \mu b^2 R - \sigma b l R$$

The strain rate is proportional to the frequency of escape:

$$\dot{\varepsilon} = A e^{-U/kT}$$

where the parameter, A, depends on the length of moving dislocation per unit volume, the density of pinning points, geometrical factors, and the frequency of vibration of a length of dislocation, l. If the yield stress is defined as the stress necessary to achieve a given strain rate, and if the preexponential terms do not vary greatly with temperature then the yield stress should vary

linearly with temperature.

$$\sigma = \frac{\nu b}{l} - \frac{kT}{blR} \ln\left(\frac{\dot{\varepsilon}}{A}\right)$$

Measurements of the yield stress at various temperatures were made for a specimen aged 10 hours, Fig. 33. From $\frac{\partial \sigma}{\partial T}$ and an extrapolation of σ to 0°K the spacing of the clusters as well as the size of the clusters necessary to give the observed hardening were calculated. The spacing between clusters, l, was found to be approximately 5×10^{-5} cm and the radius of the clusters, R, was 10Å. The initial concentration of vacancies required to form these clusters is approximately 5×10^{-7}.

Considering the uncertainty of the experimental results these values are considered to be reasonable order of magnitude estimates of the size and separation of the clusters of vacancies. The radius of the clusters revealed by small angle scattering of x-rays in quenched copper was about 25Å. This agreement is considered to be quite good and lends support to the model of Coloumb and Friedel.[14]

A model similar to that outlined above has also been given by Seeger.[23] The major difference between the model given by Seeger and that used here, is that Seeger introduces a more complicated

function for the energy to break a dislocation from a cluster of vacancies.

Quenching and aging not only raises the yield but also may affect the entire shape of the stress-strain curve. The changes in the stress-strain curve depended on the initial orientation of the crystal relative to the tensile axis. For example in a quenched and aged crystal stage I of the deformation curve was absent in crystals oriented for easy glide, while in crystals which were oriented for multiple glide, only minor changes in the work hardening were observed. A possible interpretation of these results is the following: In quenched crystals, the first dislocations which move out along the slip plane may "sweep up" or absorb clusters of vacancies in their path.[17] Subsequent movement of other dislocations on this same plane should therefore be somewhat easier. Since there would now be fewer obstacles to the motion of these dislocations. As a result, slip might be expected to occur only on a few isolated or widely-spaced slip bands in the quenched crystals. In those crystals oriented for easy glide, the stress concentrations near localized heavy slip bands would tend to promote slip on secondary slip systems, and this premature operation of a

secondary slip system could lead to an increase in the work hardening rate.

On the other hand, if only relatively few widely spaced slip bands were formed in crystals oriented for multiple glide, moving dislocations on intersecting slip systems would cut through each other less frequently in quenched than in unquenched crystals. Since the work hardening rate in stage II of the stress-strain curve is believed to be controlled by dislocation intersections, the work hardening in quenched crystals oriented for multiple glide should be less than that in unquenched crystals. This effect was not observed after intermediate aging times but was observed in the final stages of aging, as will be described below.

iii) Final Stages of Aging

The stress-strain diagrams for specimens aged for more than 10 hours after quenching from 1060°C are reproduced in Figs. 22-28, 29, and 30. The pertinent observations were the following:

a) There was a further increase in slope of the stress-strain curves below the yield stress in quenched and aged specimens, as compared to the unquenched specimens.

b) The yield stress was higher in quenched and aged specimens, than it was in the unquenched specimens.

c) However, the work hardening rate of quenched and aged crystals oriented for multiple glide was significantly less than that for unquenched crystals, and the curves now crossed, Fig. 30.

d) The yield stress for the single slip orientation crystals was initially higher than that in the unquenched samples but the curves cross at higher strains as can be seen in Fig. 22.

A mechanism has already been given to account for the first two observations, which were characteristic of both intermediate as well as longer aging times. The reduced work hardening rate in quenched crystals oriented for multiple glide was consistent with the assumption that coarse slip bands were formed in quenched crystals. If slip were highly localized on a few widely spaced bands, intersections between gliding dislocations would have been less likely to have occurred. These coarse slip bands could have continued to widen without rapid work hardening until the bands have grown to such an extent that the entire gauge length is filled.

At this point, intersection between dislocations would become important, as in unquenched crystals, thereby leading to an increase in the work hardening rate.

Conclusions

1. Since small angle scattering of x-rays was absent in freshly quenched crystals, it was concluded that,

a) Clusters of excess vacancies do not have a size larger than 8 to 10Å in radius in freshly quenched samples.

b) No appreciable deformation was introduced by quenching and no double-Bragg scattering was present.

2. Small angle scattering was observed to increase with aging and reached a maximum value after approximately 100 minutes at room temperature, from which it was concluded that clusters of vacancies grew by the absorption of excess vacancies from the matrix.

3. The small angle scattering results indicated that the shape of the clusters causing the scattering in quenched and aged crystals was approximately spherical.

4. The excess resistivity introduced by quenched crystals de-

cays in approximately 2½ hours at room temperature. In view of the small angle scattering results, it seems likely that an appreciable fraction of the excess vacancies were forming clusters rather than being annihilated at surfaces or dislocations.

5. Mechanical properties of specimens quenched from 1060°C and aged less than ten minutes at room temperature were the same as annealed specimens. It was concluded from this that isolated vacancies and small vacancy clusters do not change the mechanical properties of the crystals.

6. In quenched crystals oriented for single slip and for multiple slip aging increased the yield stress.

7. The yield stress of quenched and aged specimens was found to increase linearly with decreasing temperature.

8. Conclusions six and seven are consistent with a model advanced by Coloumb and Friedel.

9. This model, which attributes hardening observed in quenched crystals to thermal and stress assisted cutting of vacancy clusters by dislocations, allows a direct estimate to be made of the size and the separation of the clusters involved. The size and separ-

ation of the clusters were found to be 10Å and 5×10^{-5} cm, respectively. This estimated radius is in order of magnitude agreement with the cluster size measured by small angle scattering.

10. In quenched and aged crystals oriented for easy glide no easy glide was observed.

11. In quenched and aged crystals, oriented for multiple glide, the work hardening was not changed for aging times of less than 10 hours at room temperature while in quenched crystals aged for more than 10 hours the work hardening decreased.

12. The observed changes in work hardening rates in quenched crystals can possibly be explained by assuming that slip is less uniformly distributed in quenched and aged crystals than it is in annealed crystals.

13. No dislocation loops or stacking fault tetrahedra were observed in a quenched copper specimen by transmission electron microscopy, after aging <u>two years</u> at room temperature.

Acknowledgment

The author wishes to thank Prof. Washburn for the many suggestions and clarifying conversations. He would also like to acknowledge the help of Prof. Parker and Dr. Himmel in the preparation of this material. This research was supported, in part, by the National Science Foundation and in part by the Atomic Energy Commission through the Lawrence Radiation Laboratory, Inorganic Materials.

Bibliography

1. A.H. Cottrell "Vacancies and other Point Defects in Metals and Alloys", The institute of Metals, p. 1 (1958)

2. P.B. Hirsch "Phil. Mag.", 7 67, (1962)

3. N.F. Mott "Trans. A.I.M.E.", 218 962, (1960)

4. D. Kuhlmann-Wilsdorf "Phil. Mag.", 3 125, (1958)

5. J. Bauerle and J.S. Koehler "Phys. Rev.", 107 1493, (1957)

6. C. Li, J. Washburn and E. Parker "Trans. A.I.M.E.", 197 1223, (1953)

7. F. Seitz "Phys. Rev.", 79 890 (1950)

8. R. Maddin and A. Cottrell "Phil. Mag.", 46 735, (1955)

9. L. Tannor and R. Maddin "Acta Met.", 7 76, (1959)

10. M. Levy and M.Metzger "Phil. Mag." 46 1021, (1955)

11. M. Meshii and J. Kaufmann "Acta Met.", 7 180, (1959)

12. H. Kimura, R. Maddin and D. Kuhlmann-Wilsdorf "Acta Met.", 7 154, (1959)

13. H. Kimura, R. Maddin and D. Kuhlmann-Wilsdorf "Acta Met.", 7 145, (1959)

14. A. Coulomb and J. Friedel "Dislocations and Mechanical Properties of Crystals", p. 555-572, John Wiley and Sons, Inc. New York (1957)

15. D. Kuhlmann-Wilsdorf "Phil. Mag.", 3 130, (1958)

16. H. Kroupa "Phil. Mag.", 7 167, (1962)

17. G. Saada and J. Washburn To be published.

18. J. Weertman "Phys. Rev.", 119 1871, (1960)

19. A. Guinier, G. Fournet, C. Walker and K. Yudovitch "Small Angle Scattering of X-rays", John Wiley and Sons, Inc. New York (1955)

20. R. Garwin "Rev. of Sci. Instr.", 29 223 (1958)

21. L. Rayleigh "Phil. Mag.", 6 37, (1919)

22. O. Kratky and O. Porod "Rec. Trav. Chim.", 68 1106, (1949)

23. J. Silcox and P. Hirsch "Phil. Mag.", 4 72, (1959)

24. H. Wilsdorf and D. Kuhlmann-Wilsdorf "Jour. of App. Physics", 31 516, (1960)

25. A. Seeger, S. Mader, and J. Diehl "Proc. European Conference on Electron Microscopy", paper J-11

26. J. Smallman, H. Westmacott "Jour. of App. Physics", 30 603, (1959)

27. W. Schule, A. Seeger, D. Schumacher, and K. King "Physica Status Solidi", 2 1199, (1962)

List of Figures

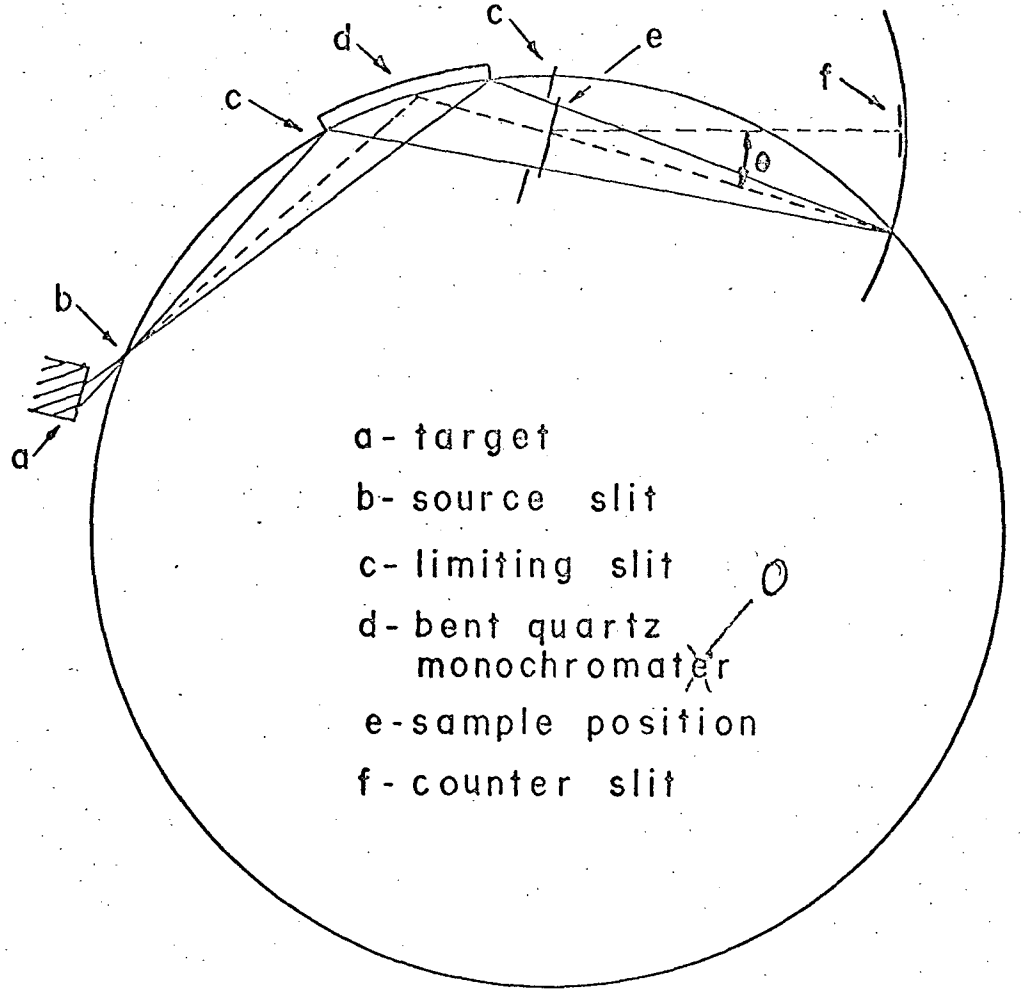
d
c
c
e
f
θ
b
a
a- target
b- source slit
c- limiting slit
d- bent quartz monochromater
e- sample position
f- counter slit
O

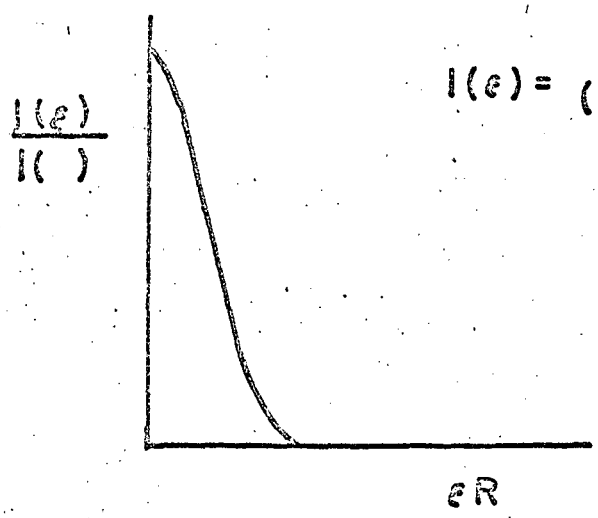

$$I(\varepsilon) = \left(\frac{3\sin\varepsilon R - R\cos\varepsilon R}{\varepsilon^3 R^3}\right)^2$$

a. Scattered intensity from a sphere of radius R versus angle, ε

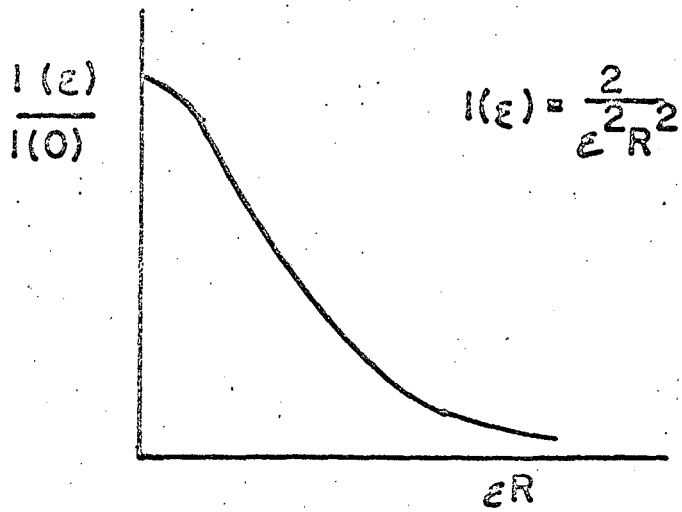

$$I(\varepsilon) = \frac{2}{\varepsilon^2 R^2}\left(1 - \frac{J_1(2\varepsilon R)}{\varepsilon R}\right)$$

b. Scattered intessity from a flat disc of radius R versus angle, ε

Figure 2 Comparison of Scattered Intensity for SPheres and Discs

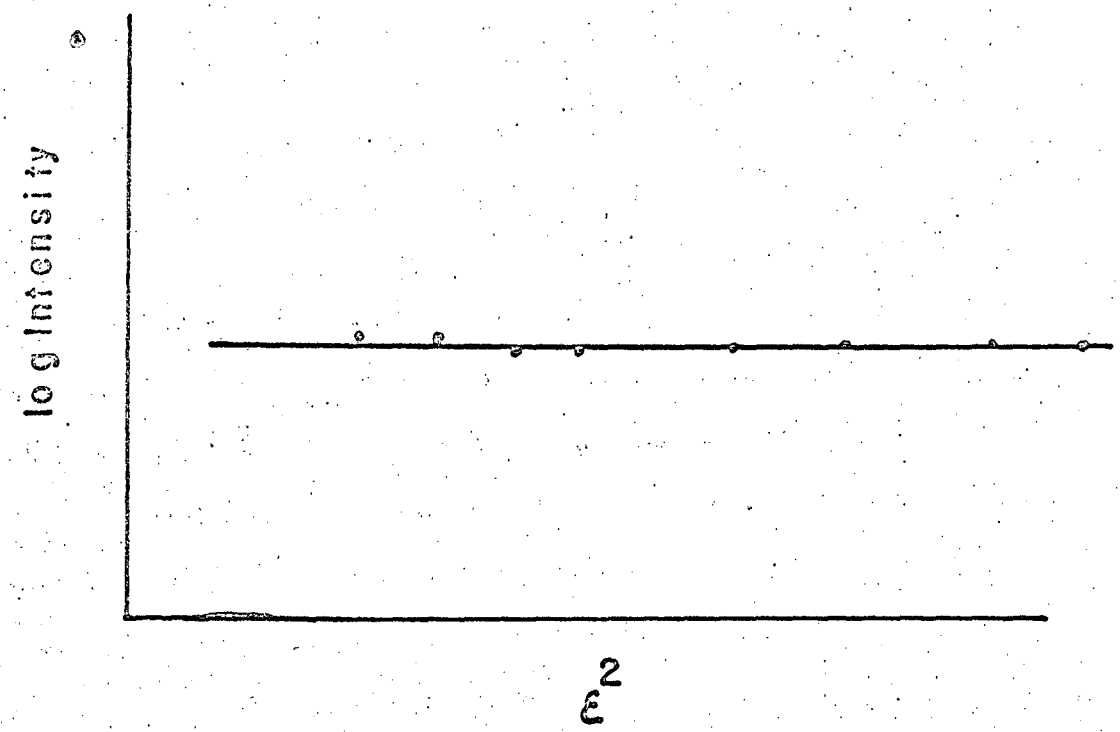

a) Initial scattering for fast quench

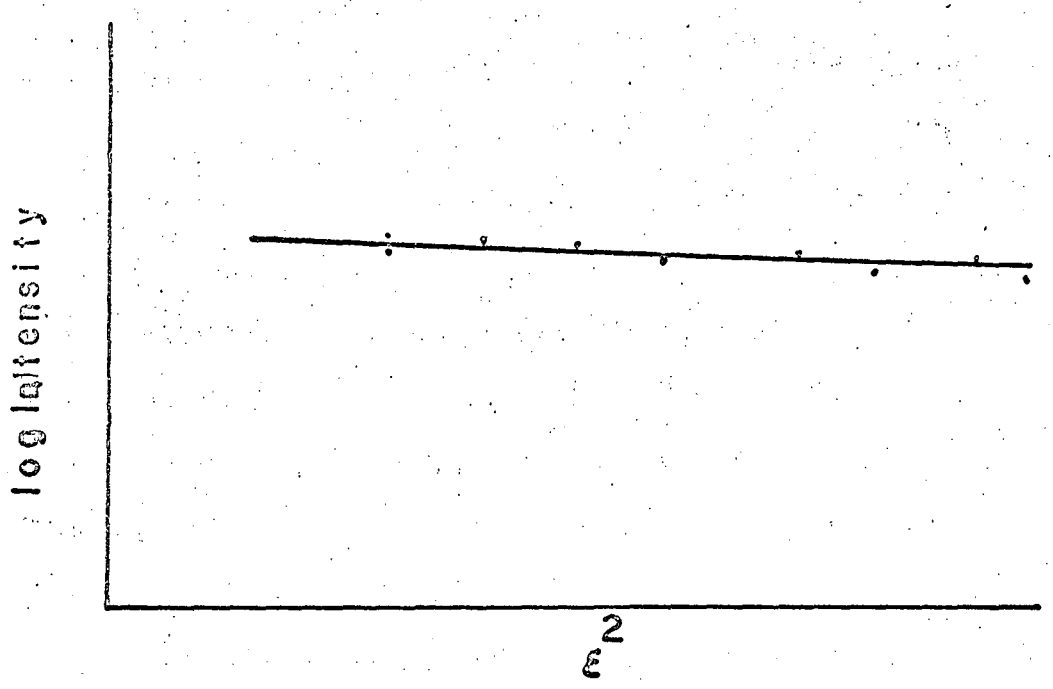

b) Initial scattering for slow quench

Figure 3 Comparison of initial scattering for slow and fast quenches

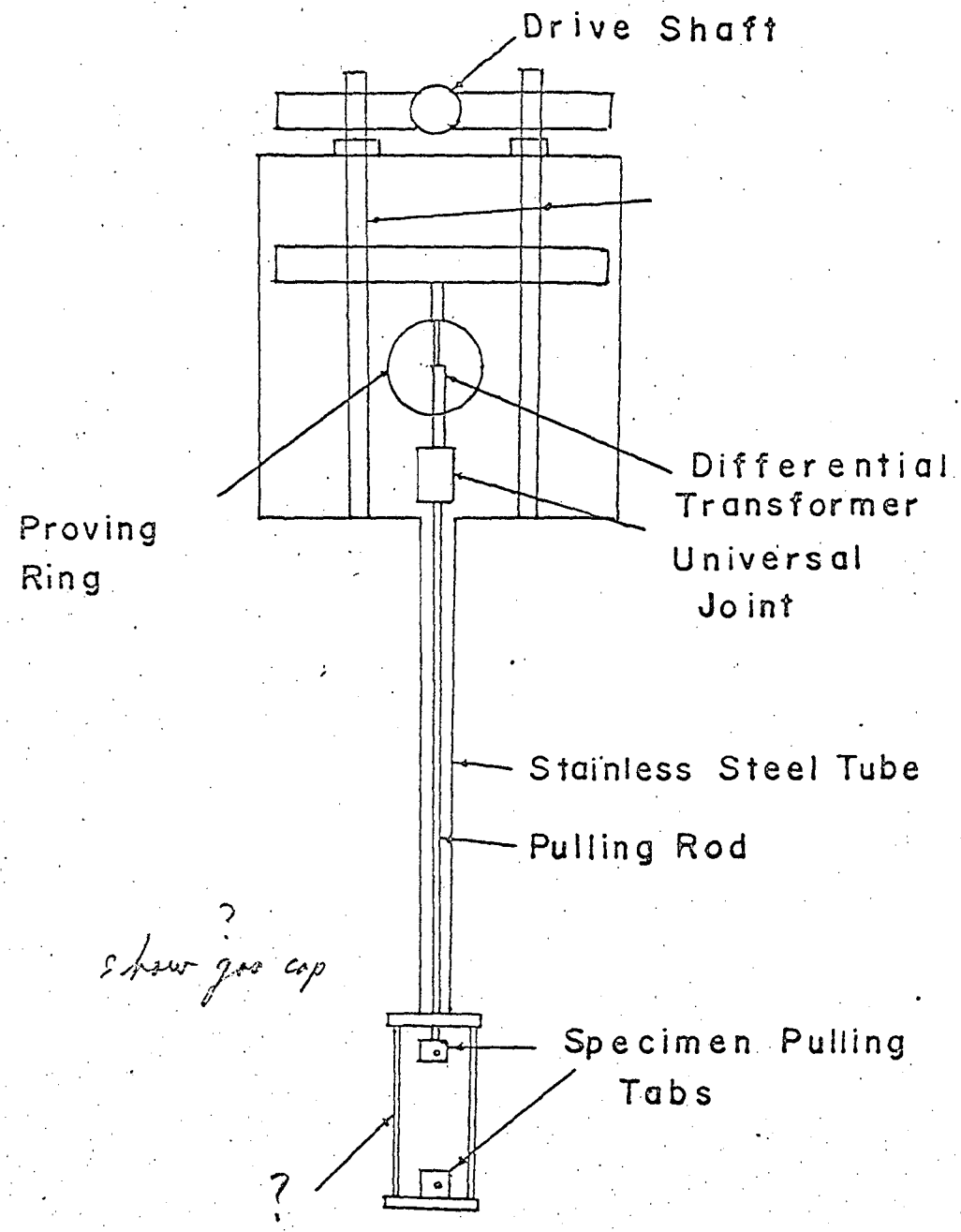

Figure 4-

Tensile Machine (Schematic)

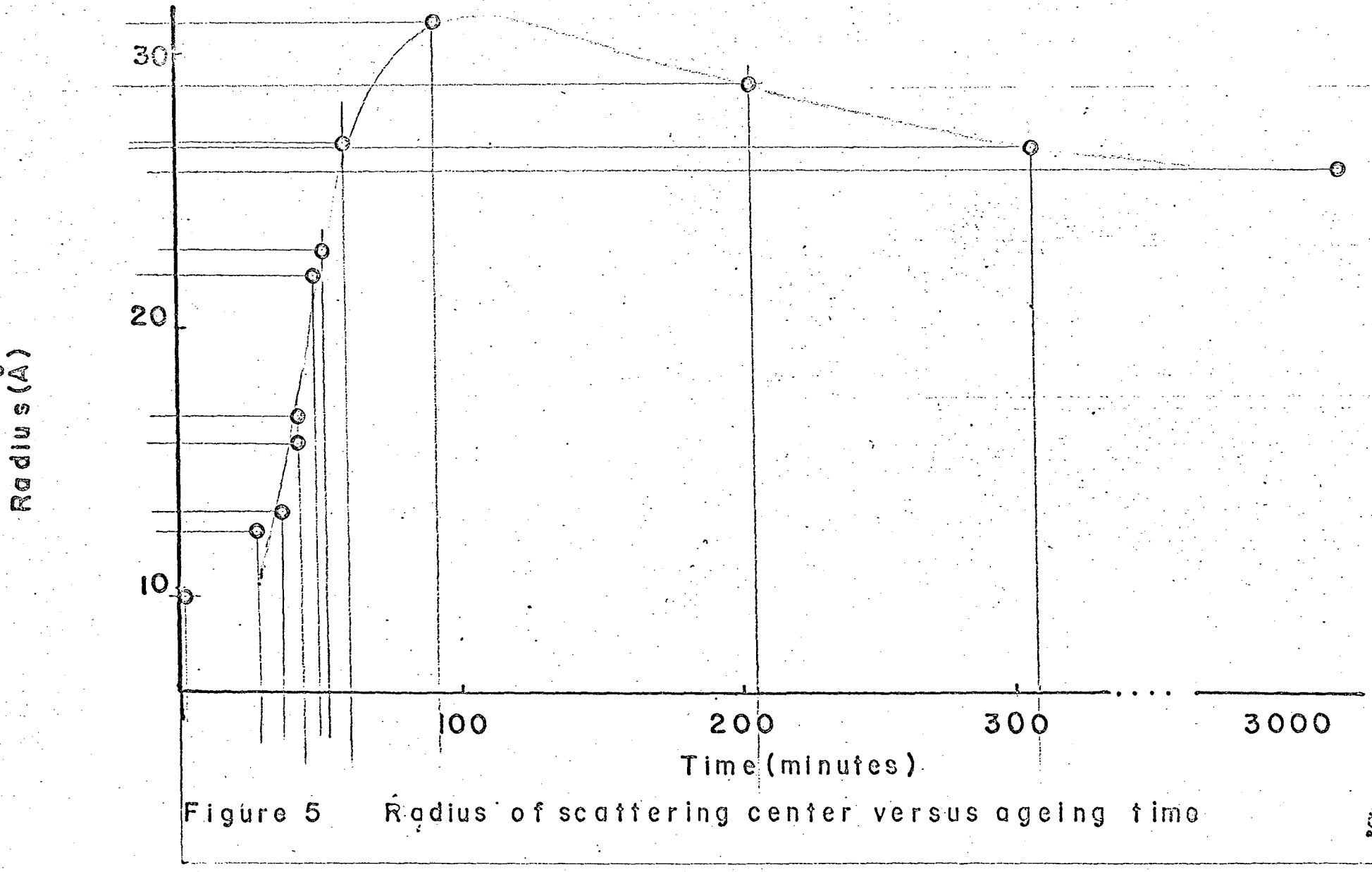

Figure 5 Radius of scattering center versus ageing time

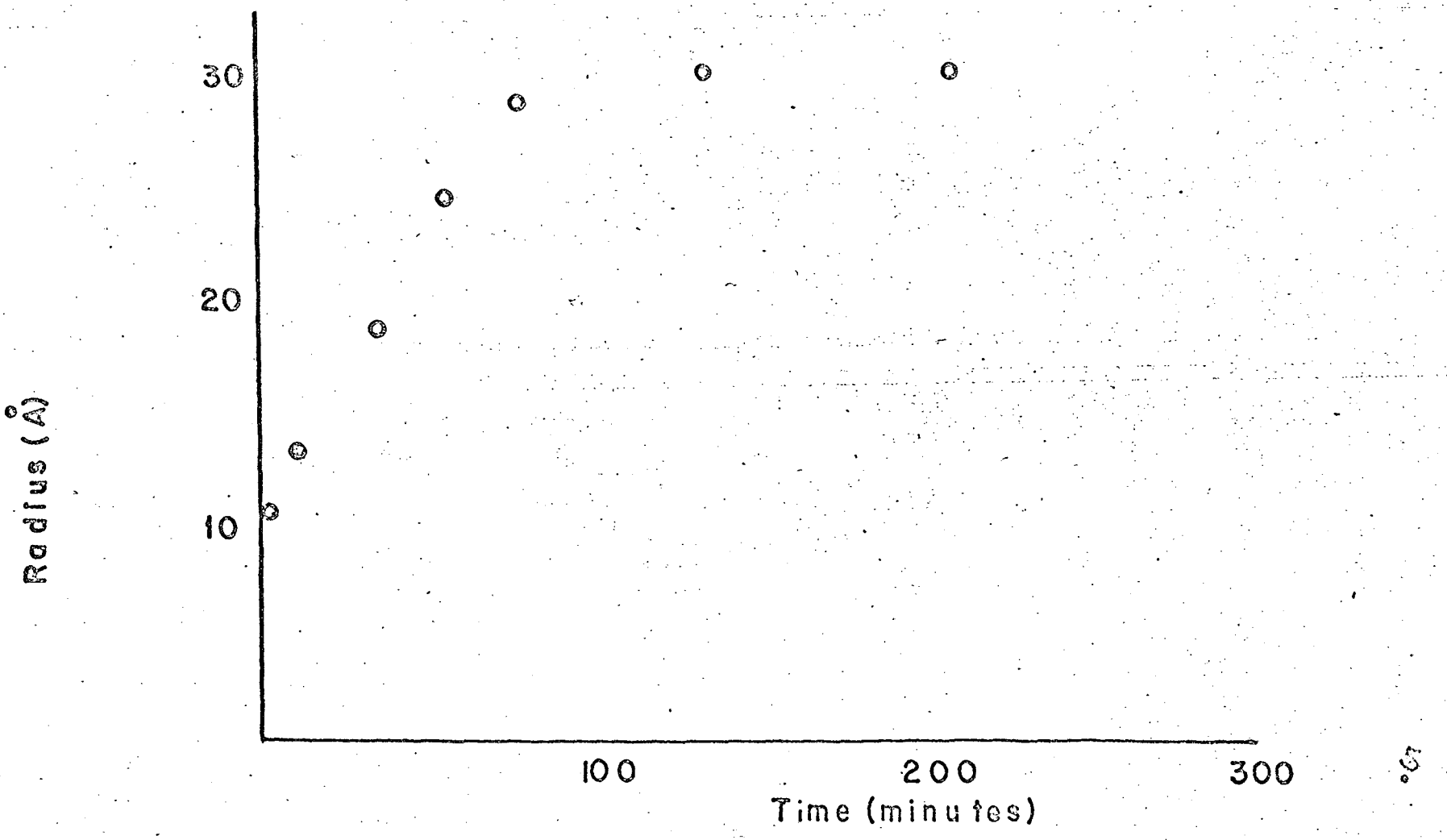

Figure 6 Radius of scattering center versus ageing time

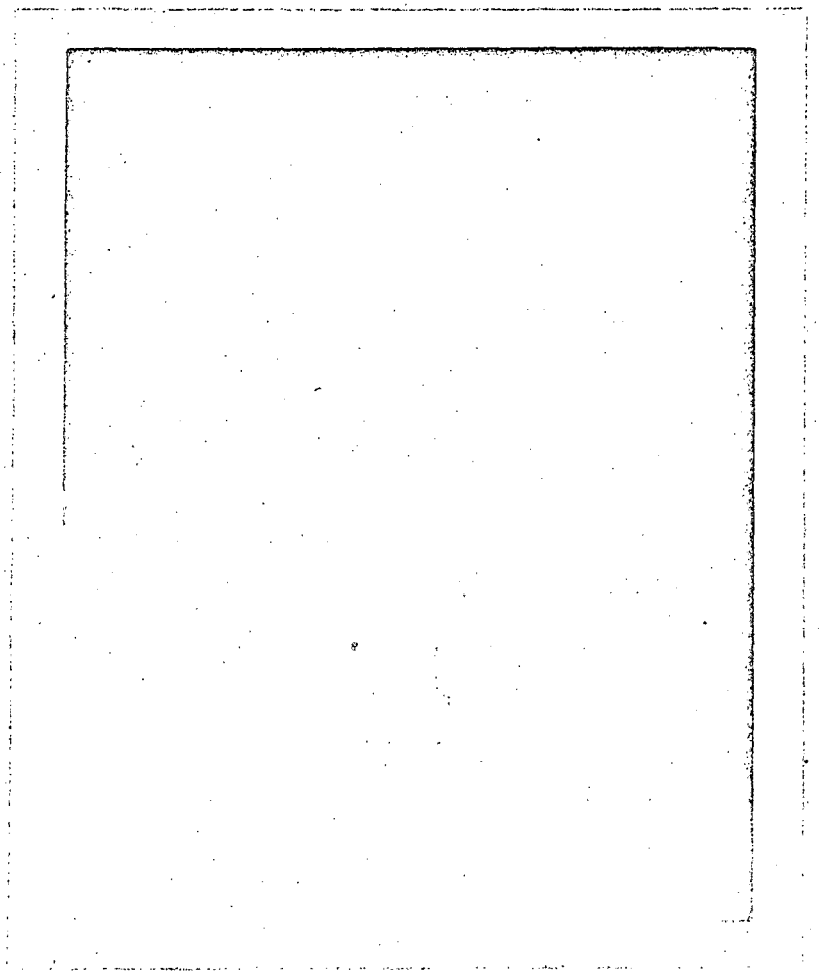

Figure 7 Electron micrograph of quenched copper aged 2 years

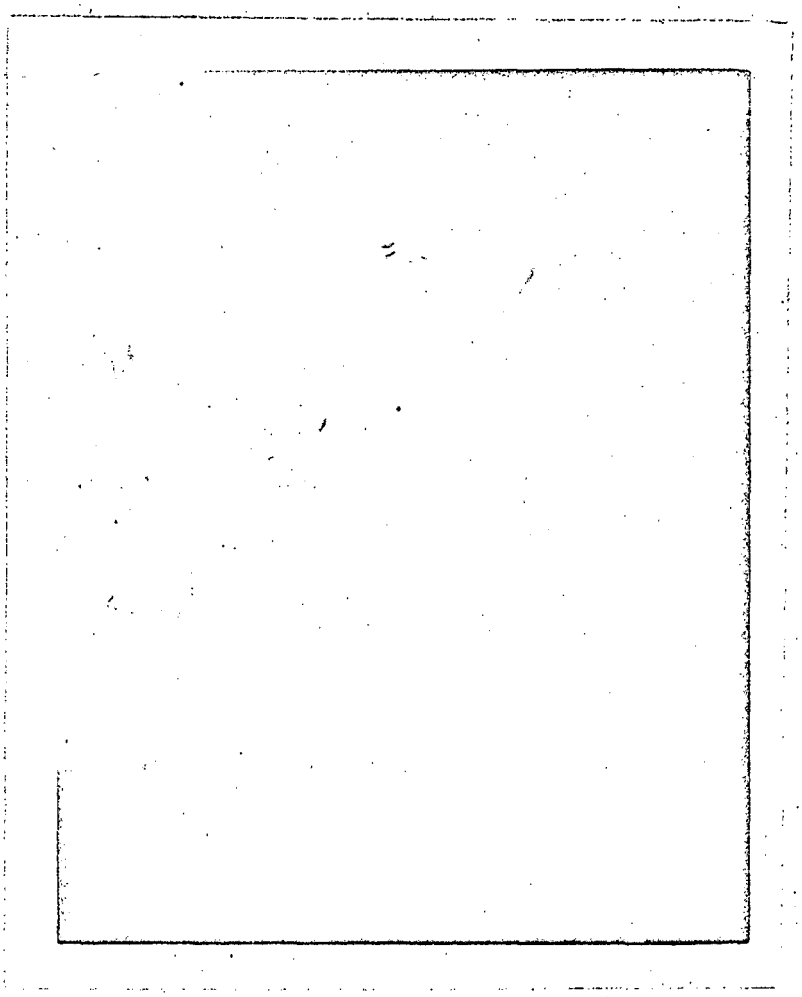

Figure 8 Electron micrograph of quenched copper aged 2 years

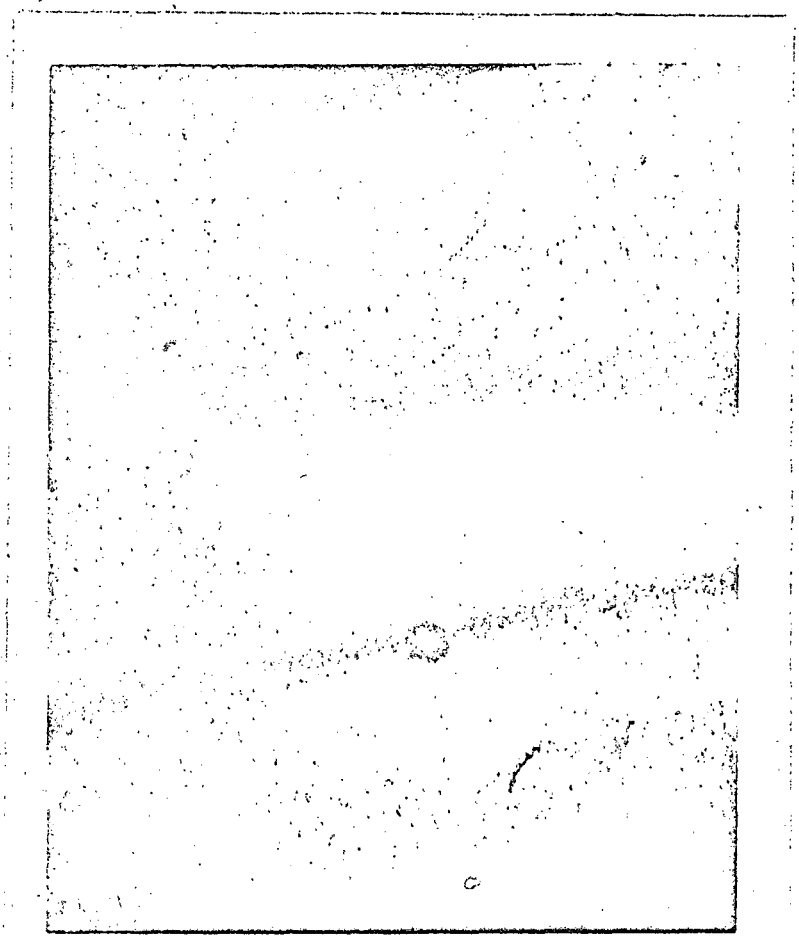

Figure 9 Electron micrograph of quenched gold

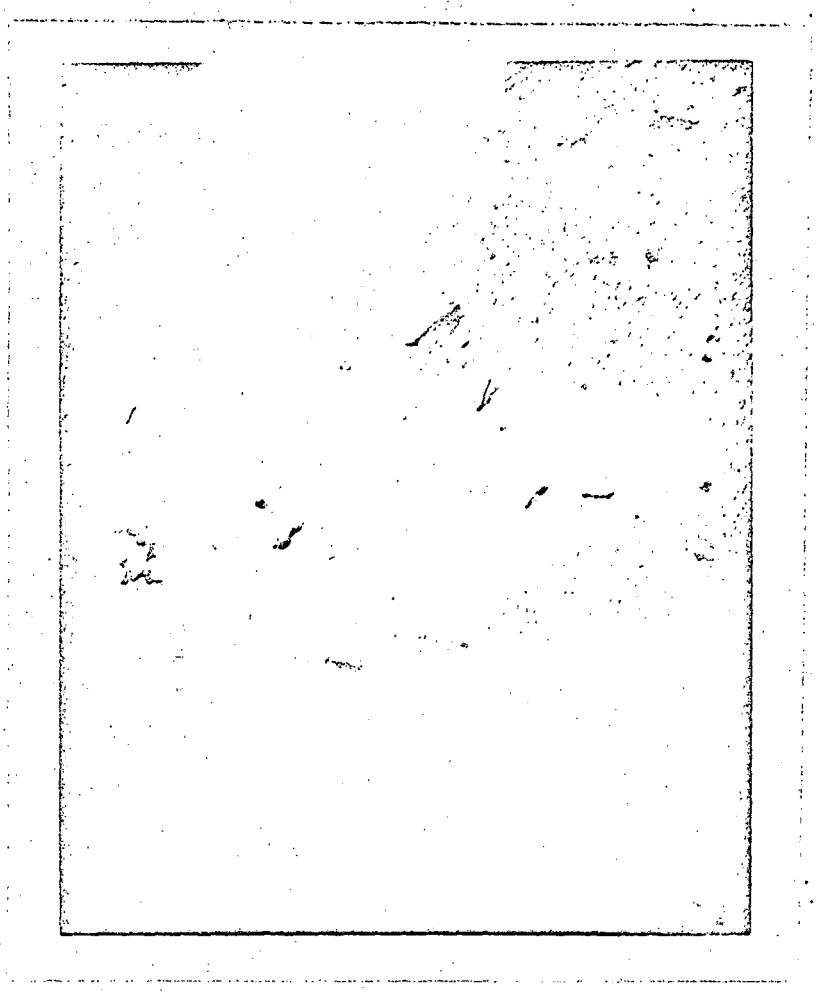

Figure 10 Electron micrograph of quenched gold

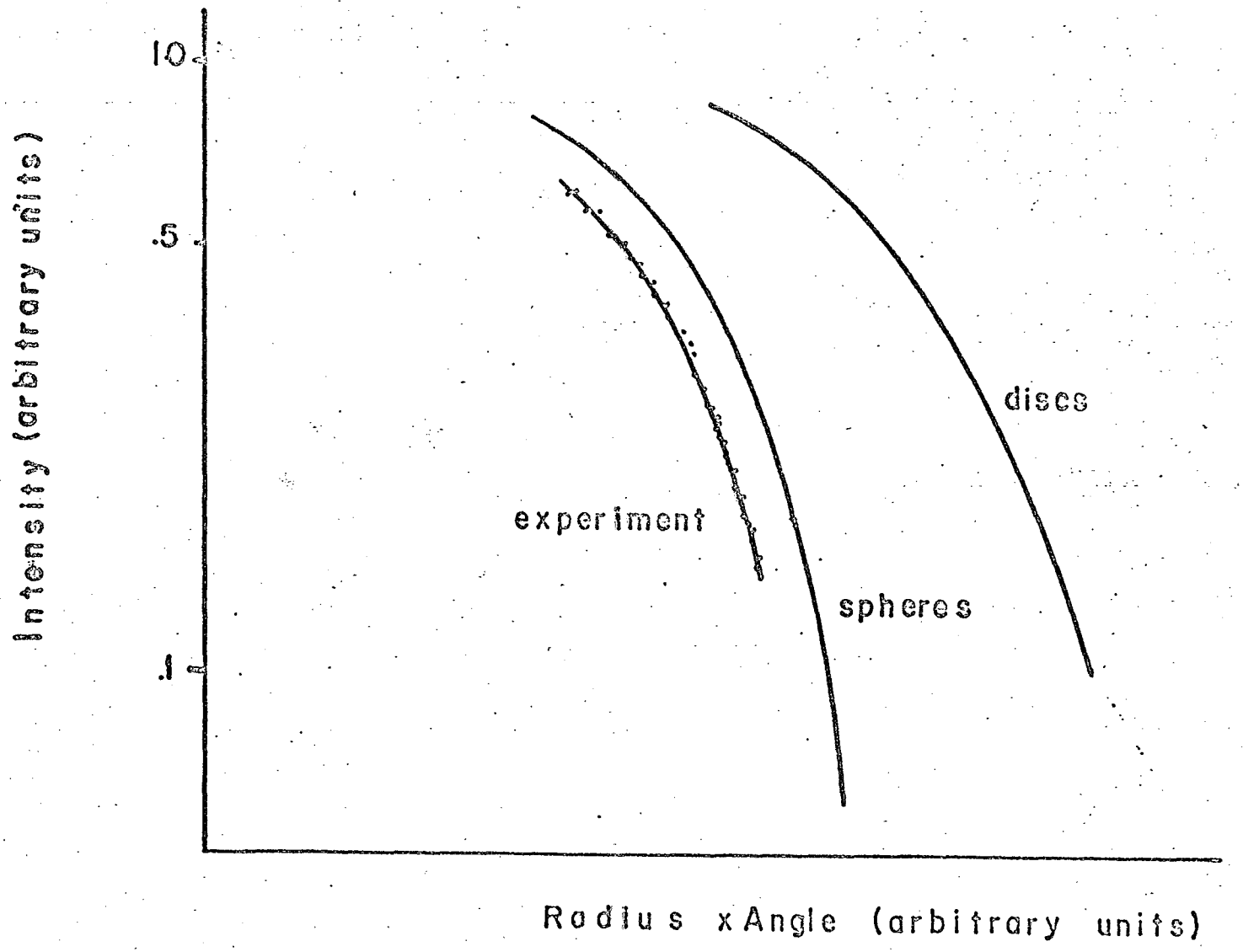

Figure II Comparison of observed intensity with calculated values for spheres and discs

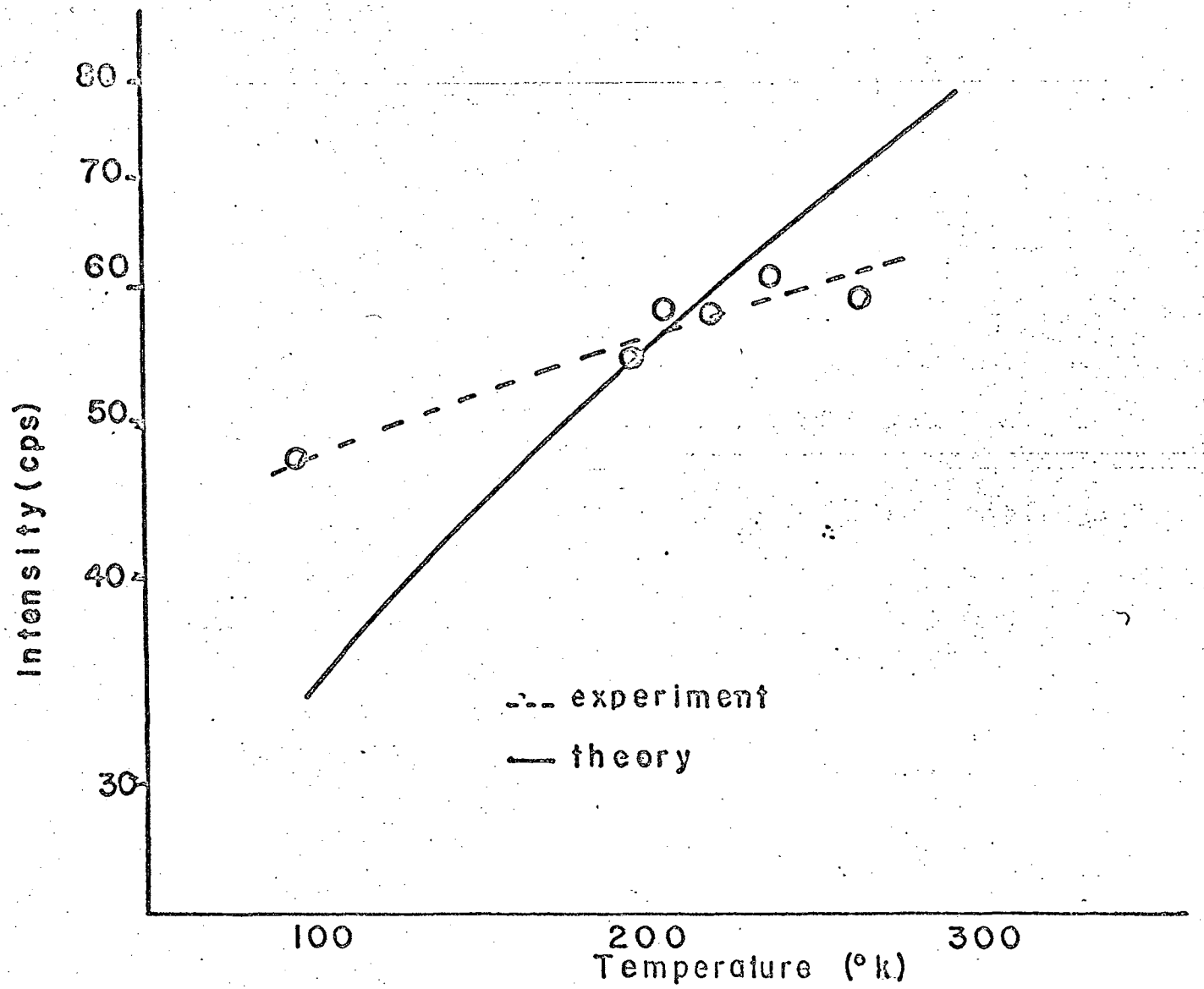

Figure 12 Temperature dependence of scattering

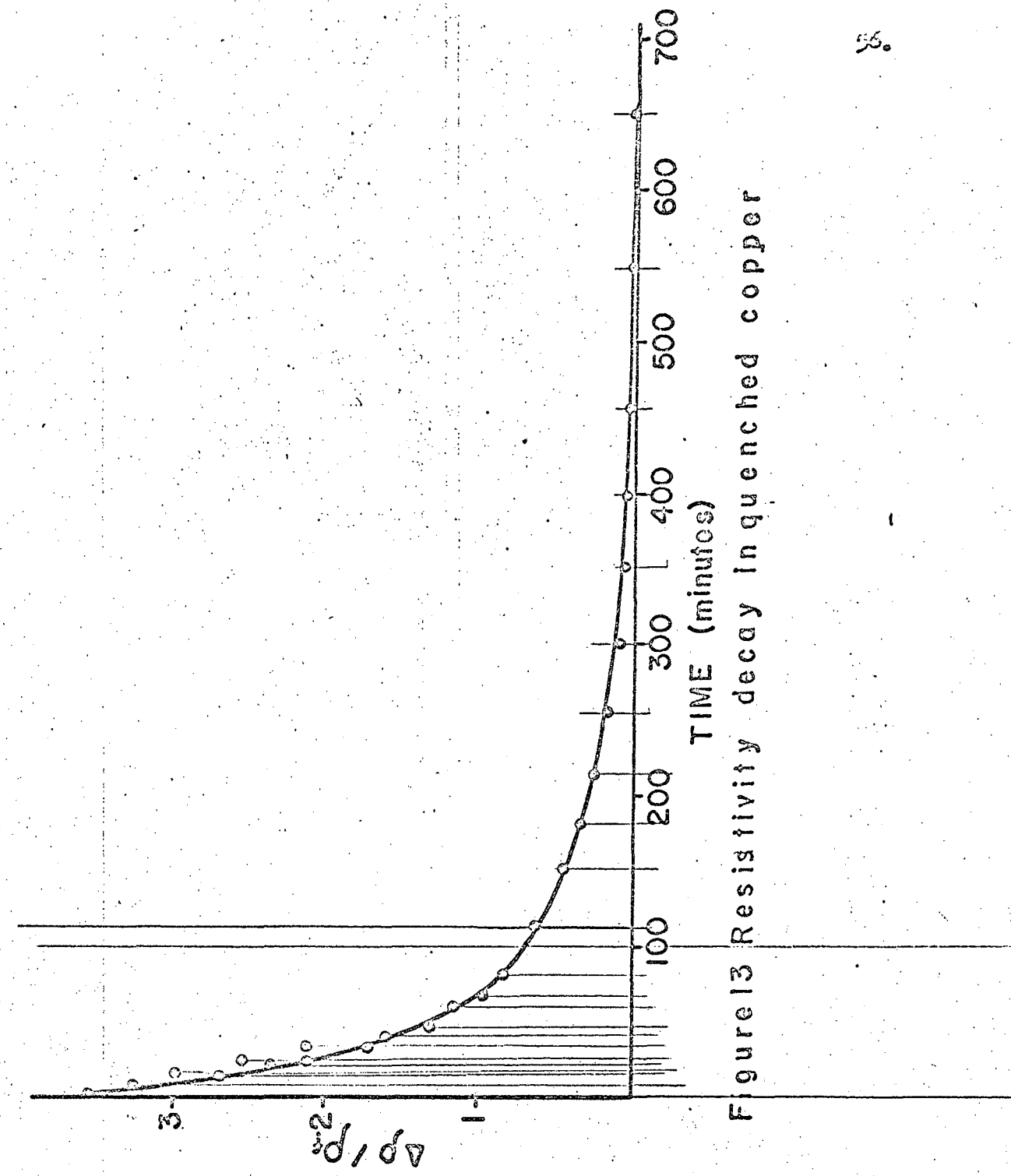

Figure 13 Resistivity decay in quenched copper

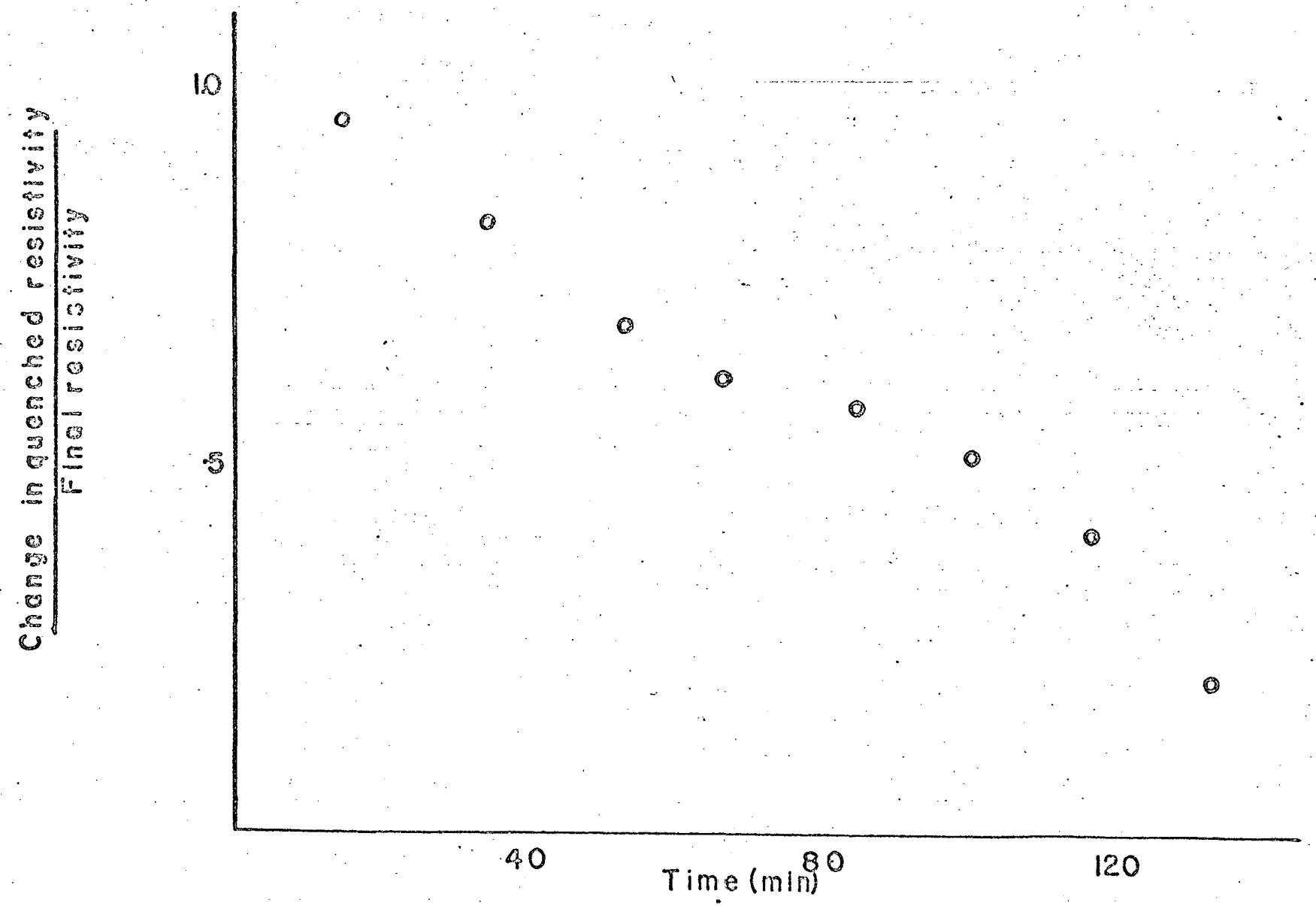

Figure 14 Resistivity decay in quenched copper

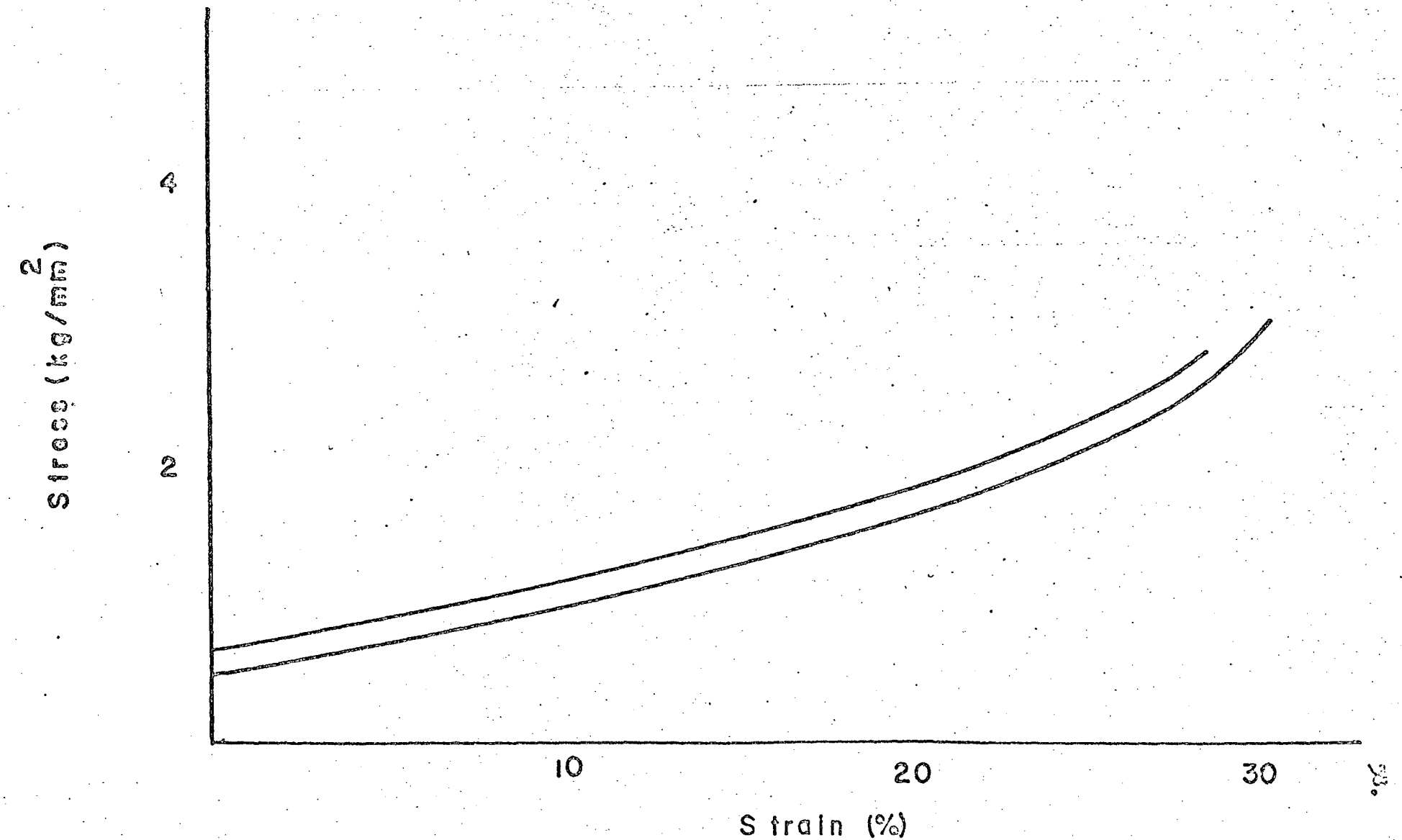

Figure 15 Stress-Strain curve for specimen oriented for single slip. Specimen aged 7 minutes at room temperature

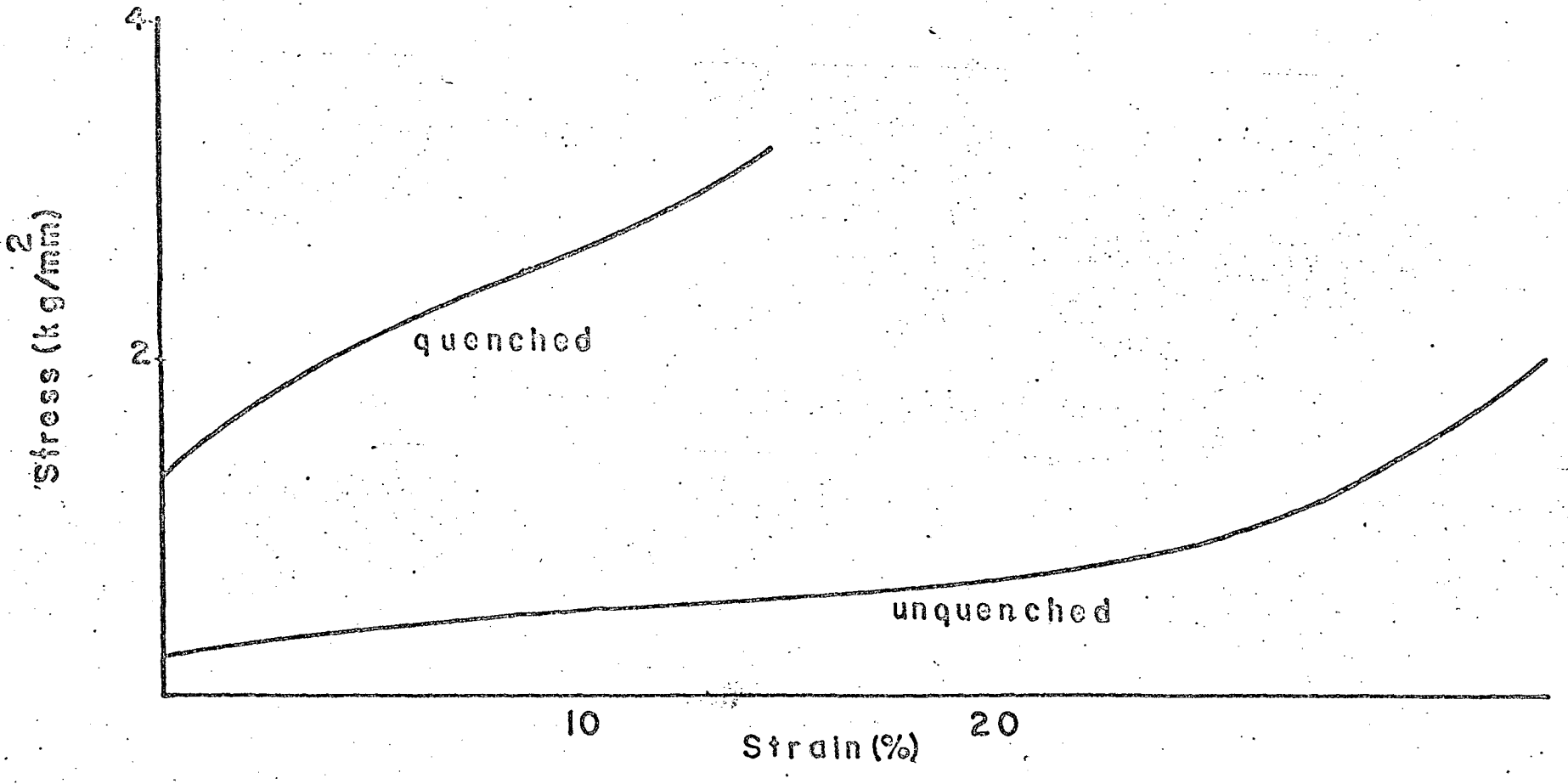

Figure 16 Stress - Strain curve for specimen oriented for single slip. Specimen aged 12 minutes at room temperature

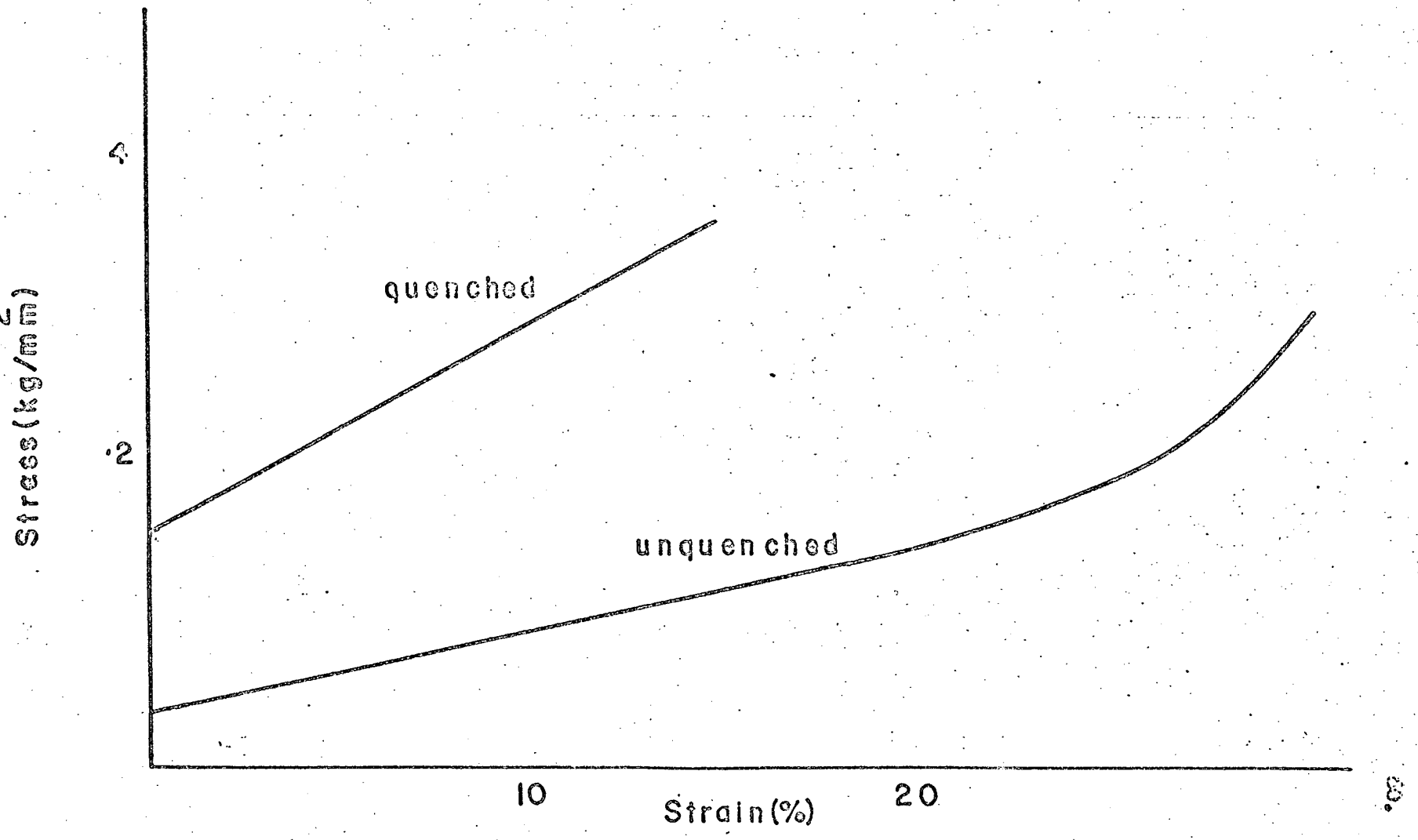

Figure 17 Stress-Strain curve for specimen oriented for single slip. Specimen aged 16 minutes at room temperature.

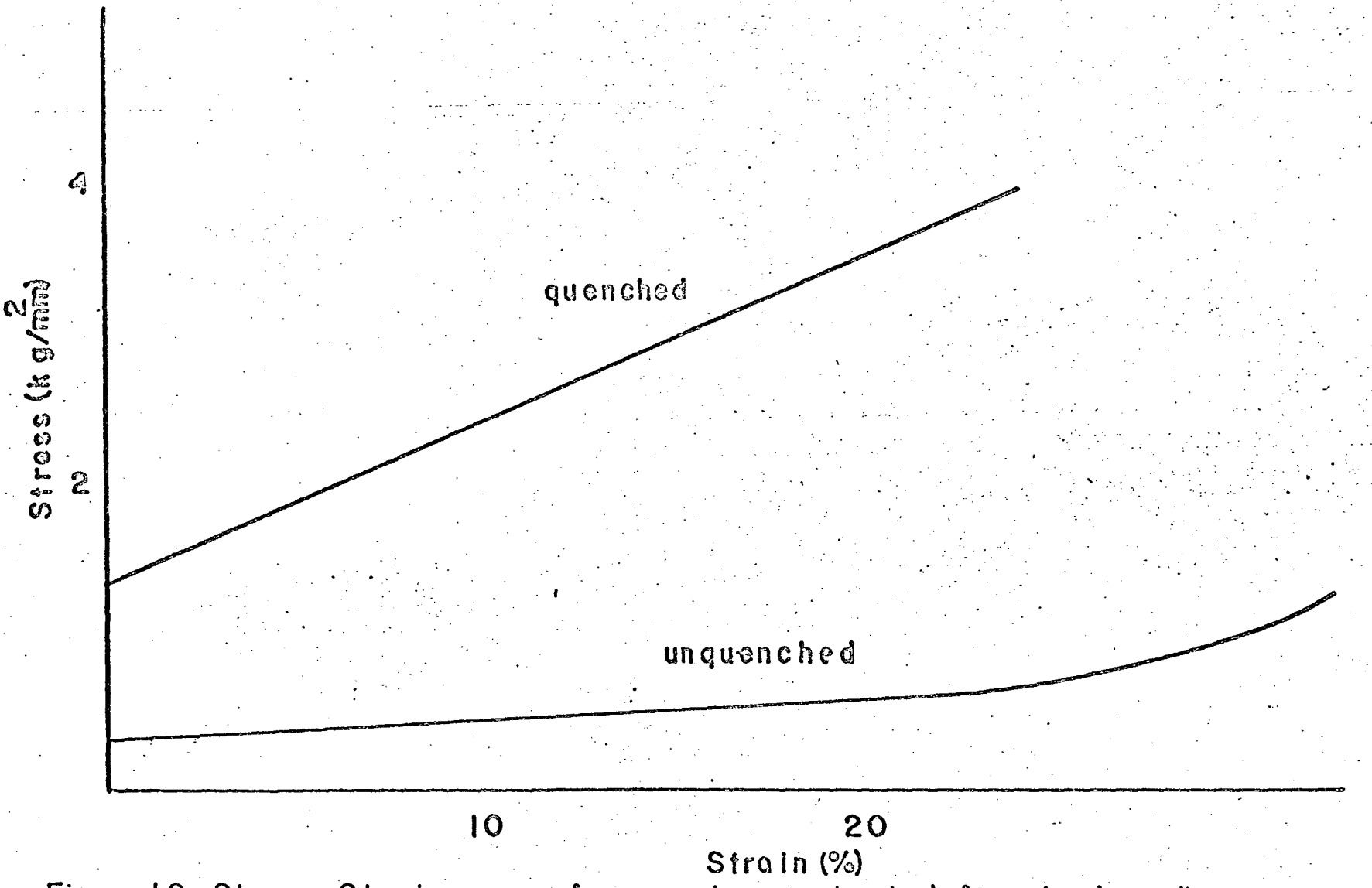

Figure 18. Stress-Strain curve for specimen oriented for single slip. Specimen aged 38 minutes at room temperature

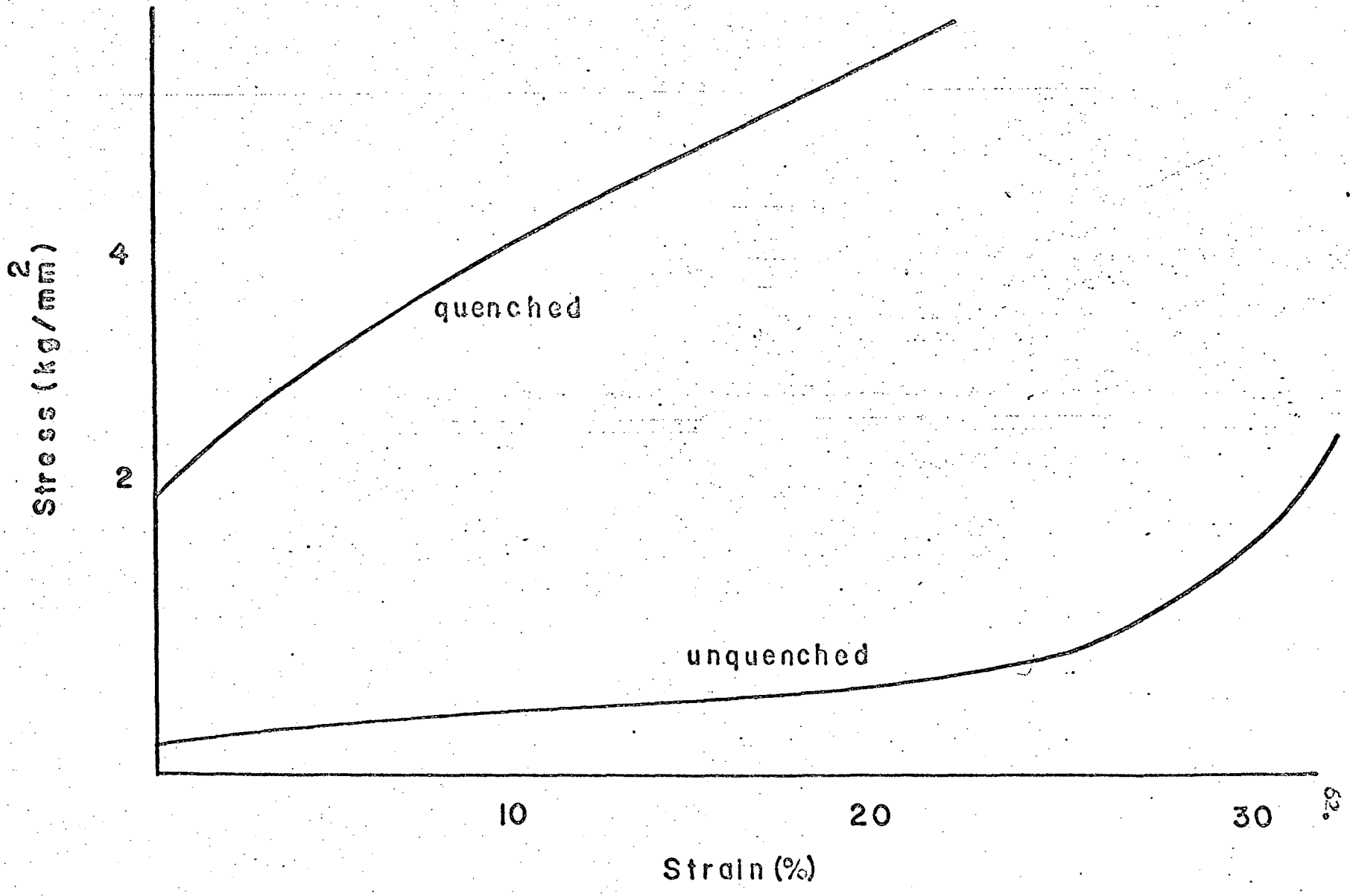

Figure 19 Stress-Strain curve for specimen oriented for single slip
Specimen aged 58 minutes at room temperature.

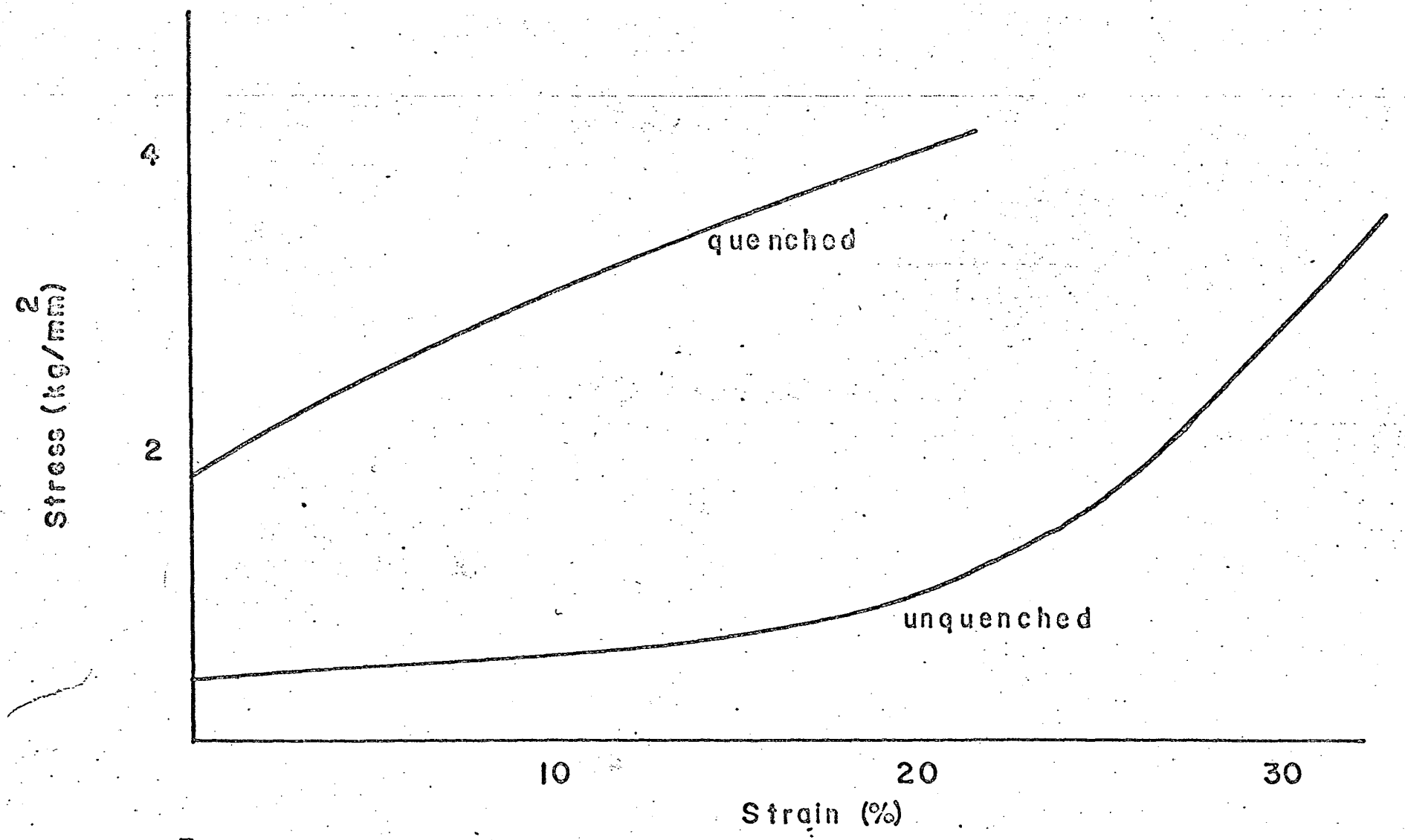

Figure 20 Stress-Strain curve for specimen oriented for single slip. Specimen aged 4 hours at room temperature.

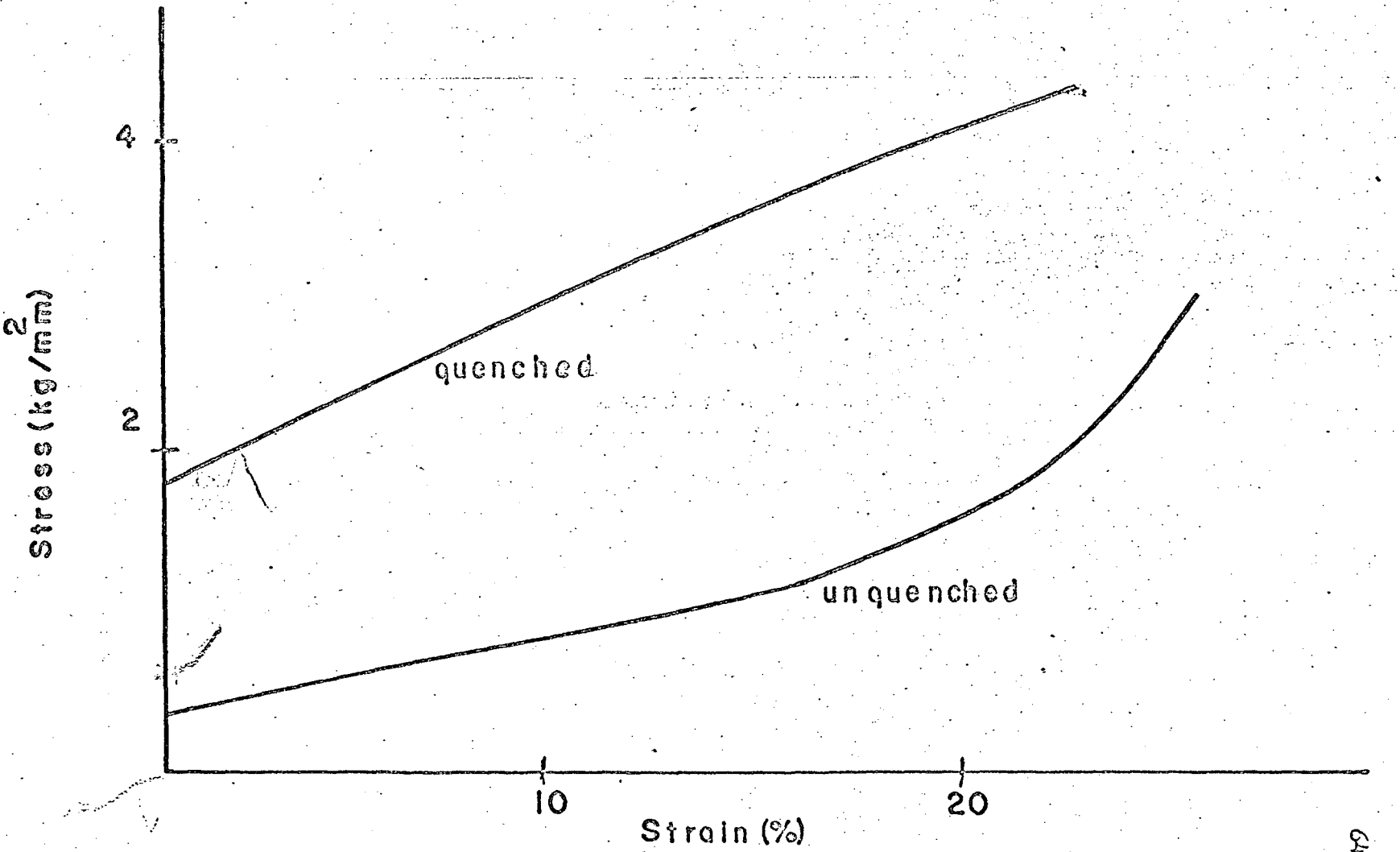

Figure 21 Stress-Strain curve for specimen oriented for single slip.

Specimen aged 10 hours at room temperature.

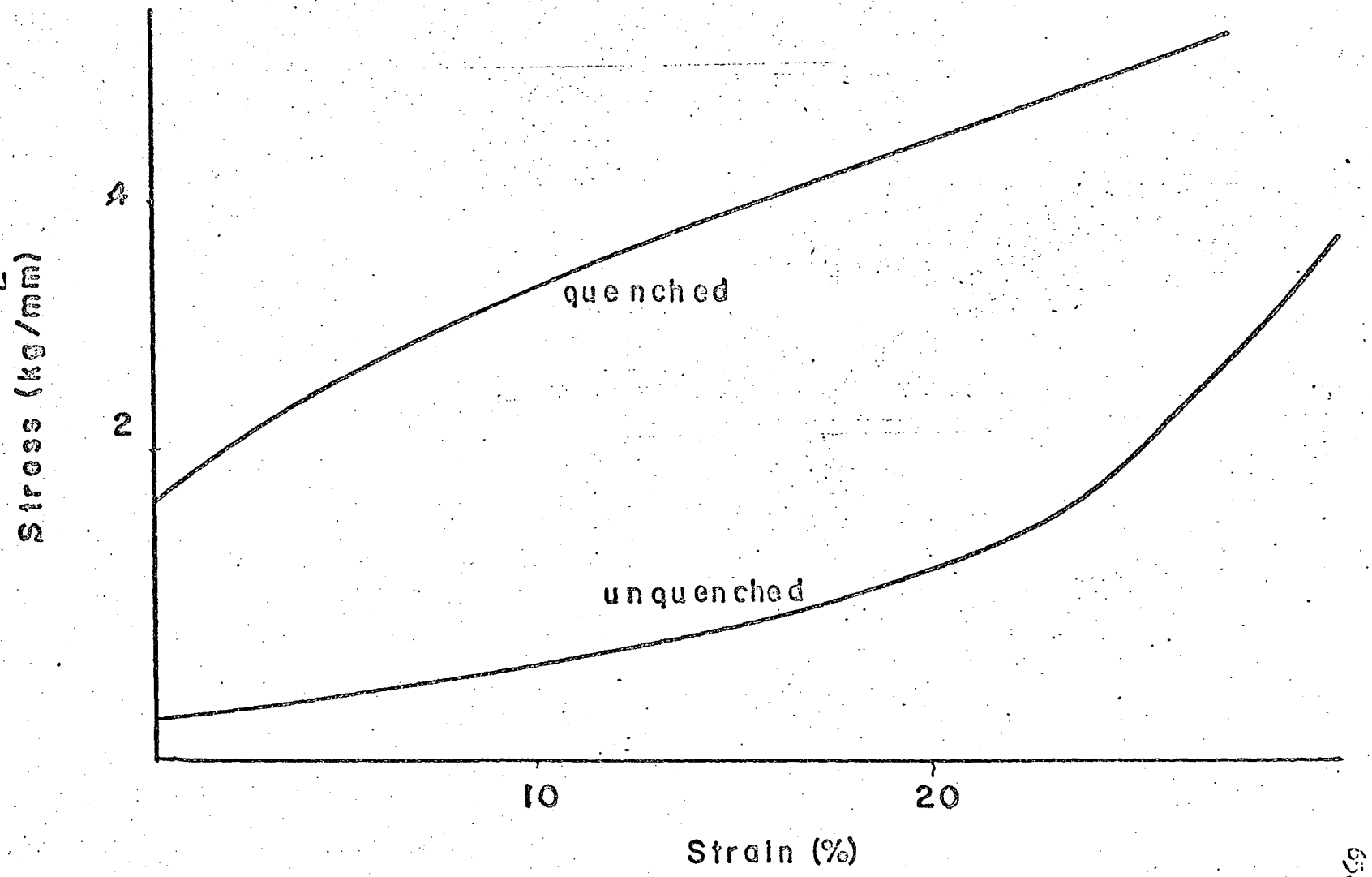

Figure 22 Stress-Strain curve for specimen oriented for single slip. Specimen aged 2 weeks at room temperature.

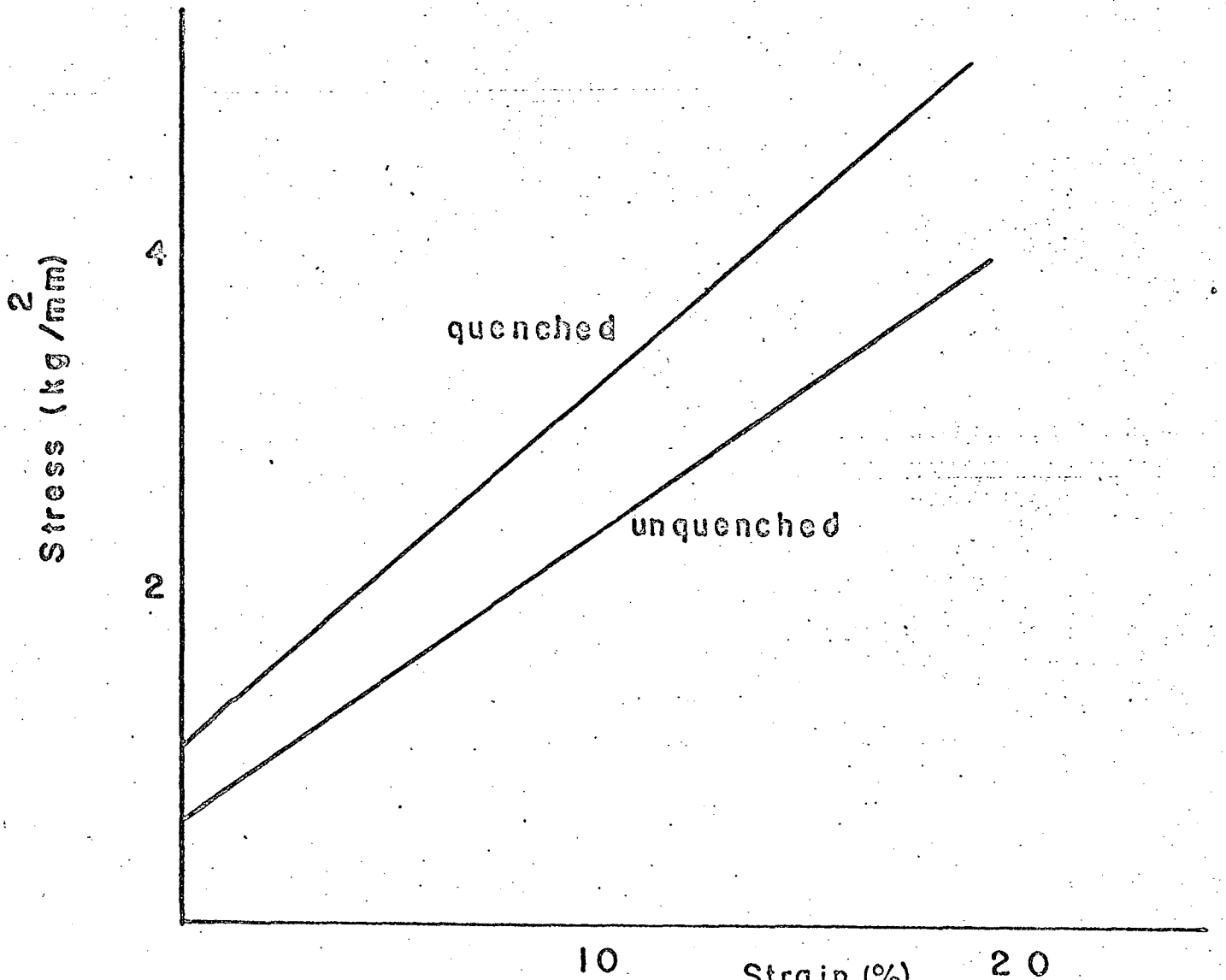

Figure 23 Stress-Strain curve for specimen oriented for multiple slip. Specimen aged 7 minutes at room temperature.

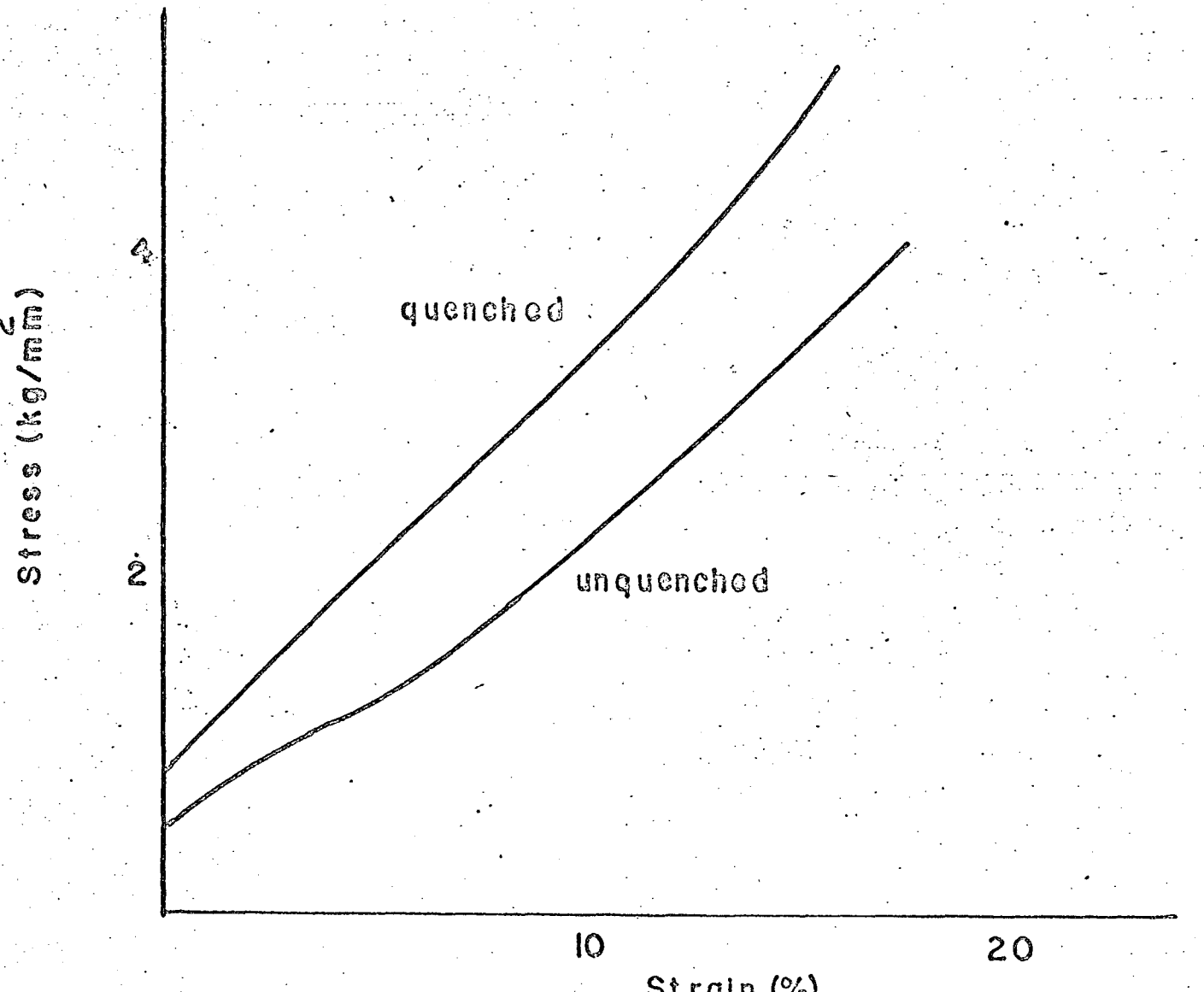

Figure 24 Stress-Strain curve for specimen oriented for multiple slip. Specimen aged 10 minutes at room temperature.

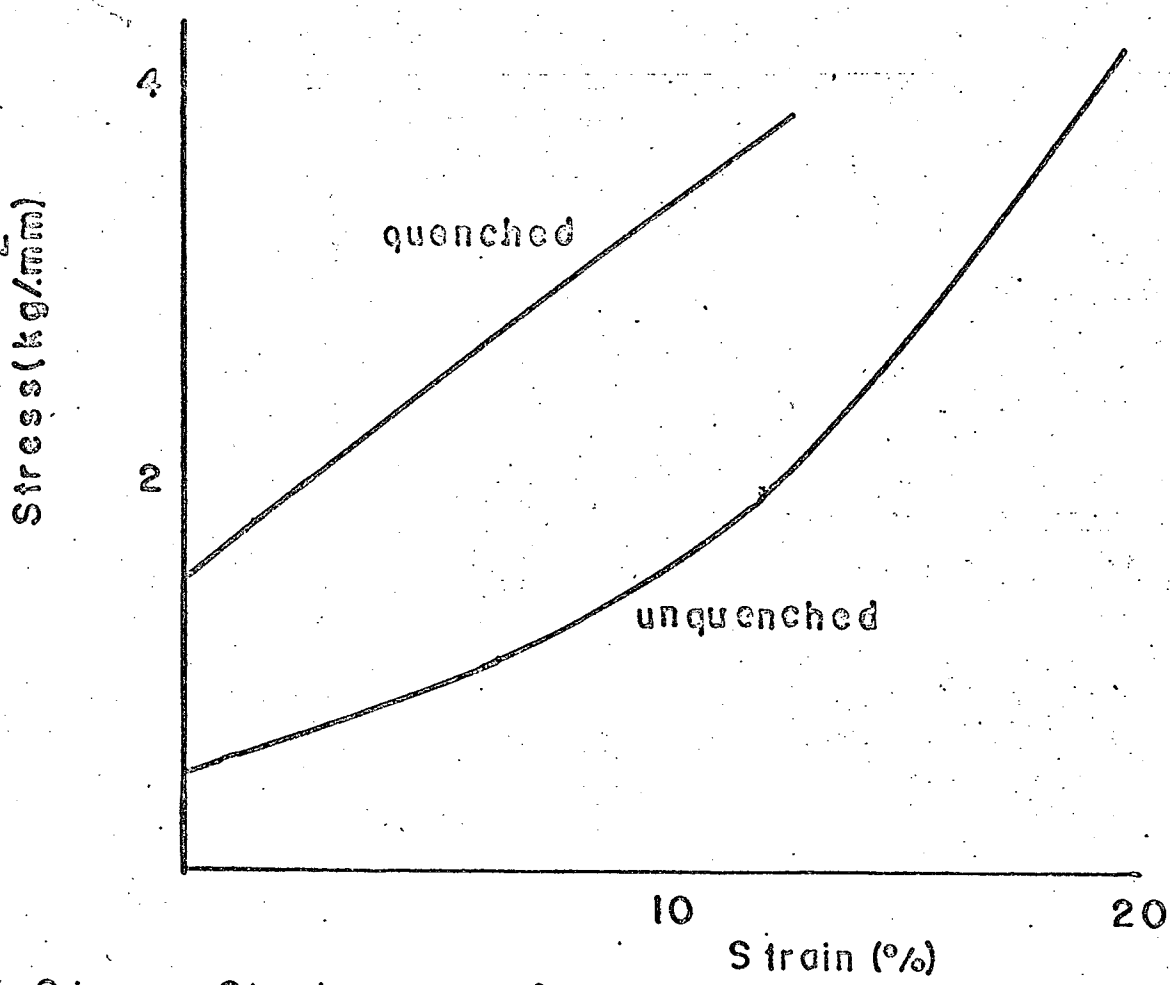

Figure 25 Stress-Strain curve for specimen oriented for multiple slip. Specimen aged 35 minutes at room temperature.

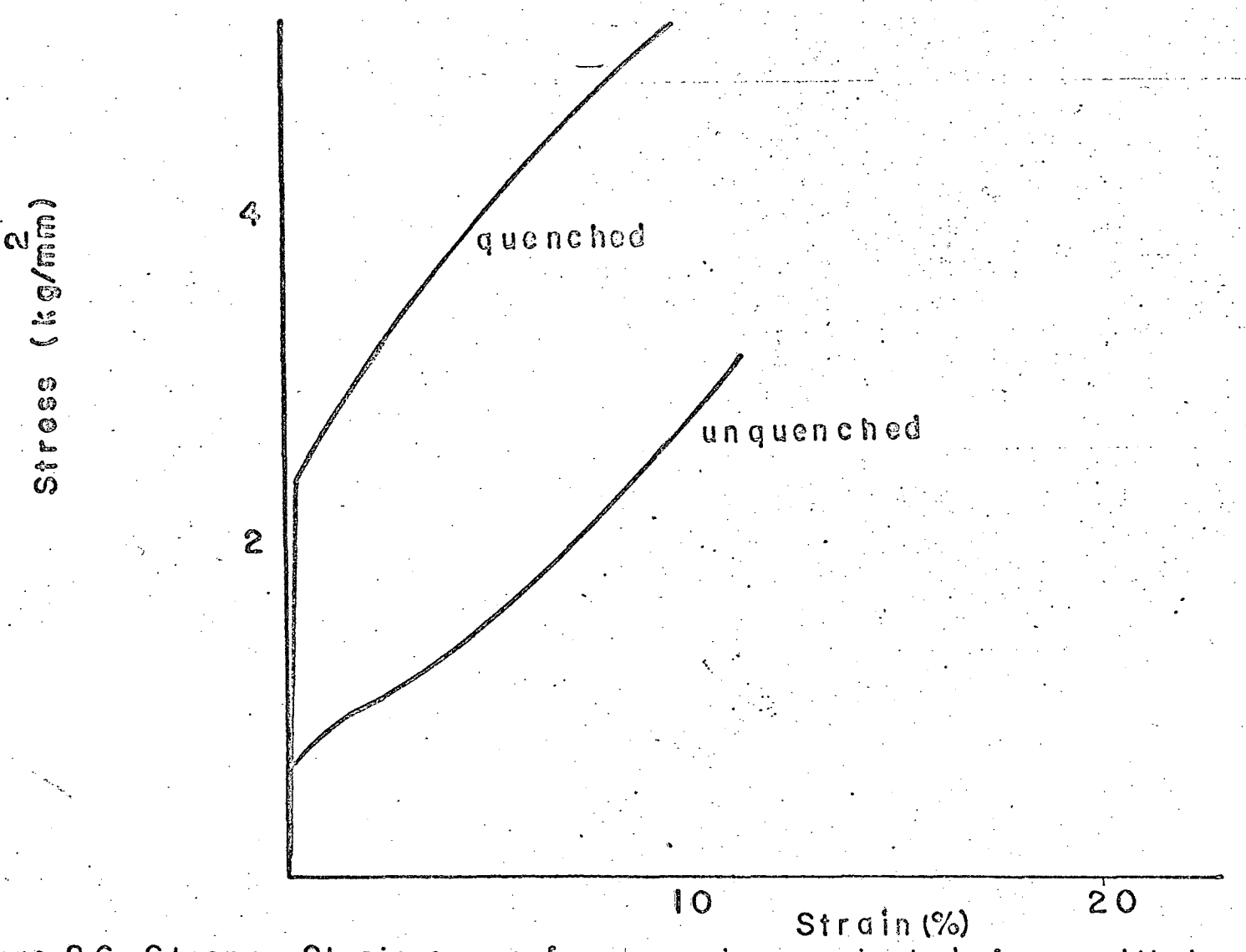

Figure 26 Stress–Strain curve for specimen oriented for multiple slip. Specimen aged 2 hours at room temperature.

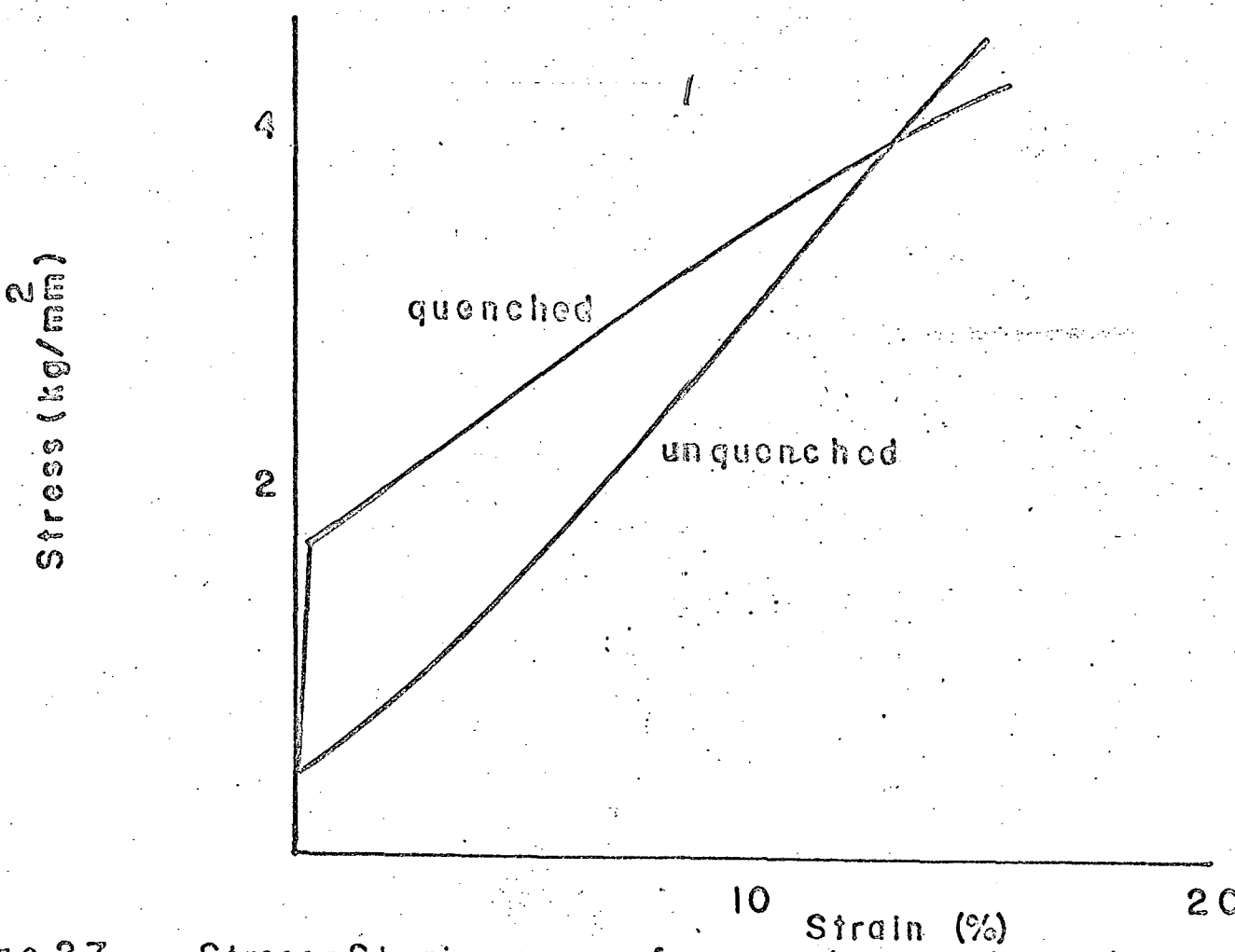

Figure 27 Stress-Strain curve for specimen oriented for multiple slip. Specimen aged 6 hours at room temperature

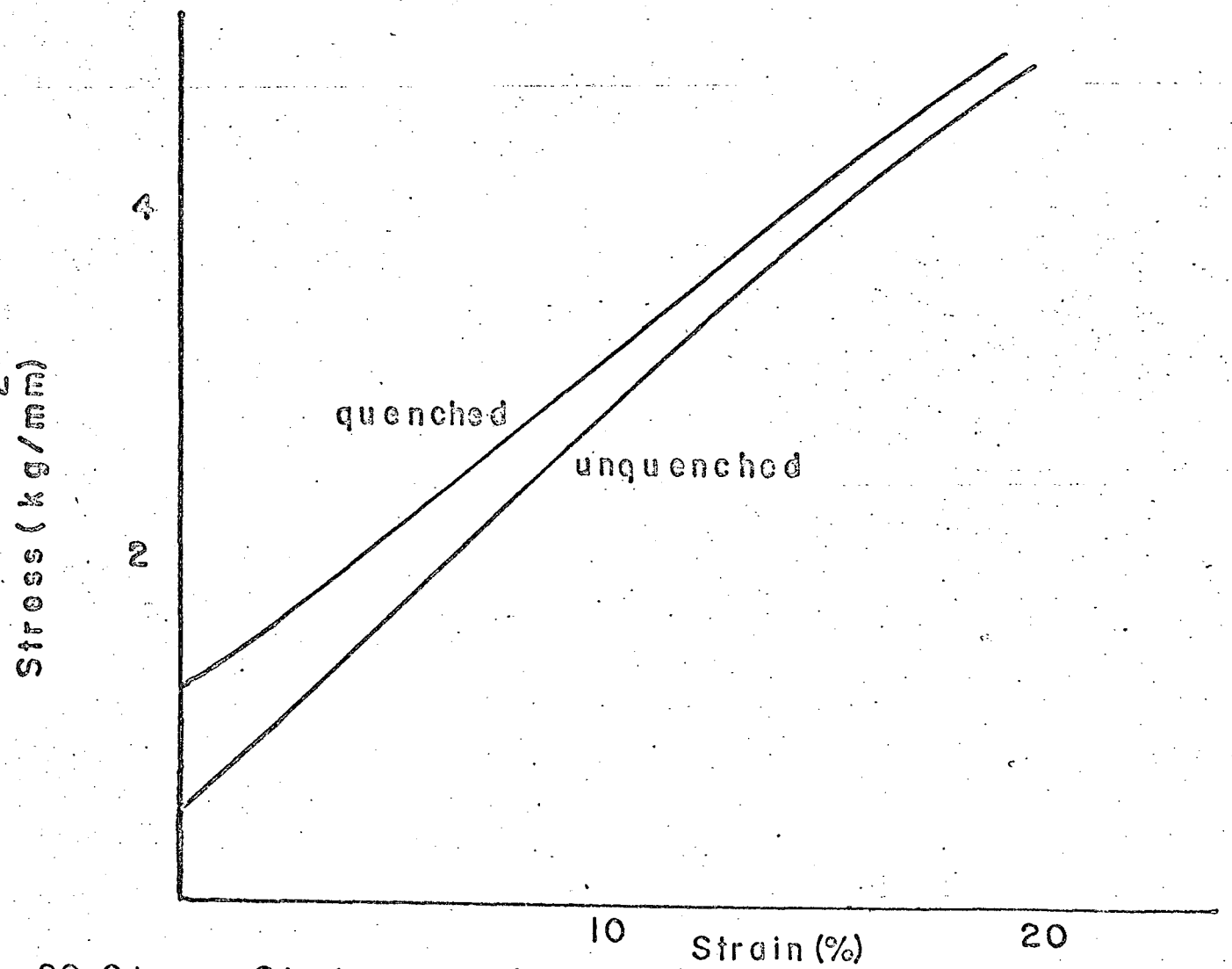

Figure 28 Stress-Strain curve for multiple slip specimen aged 10 hours at room temperature.

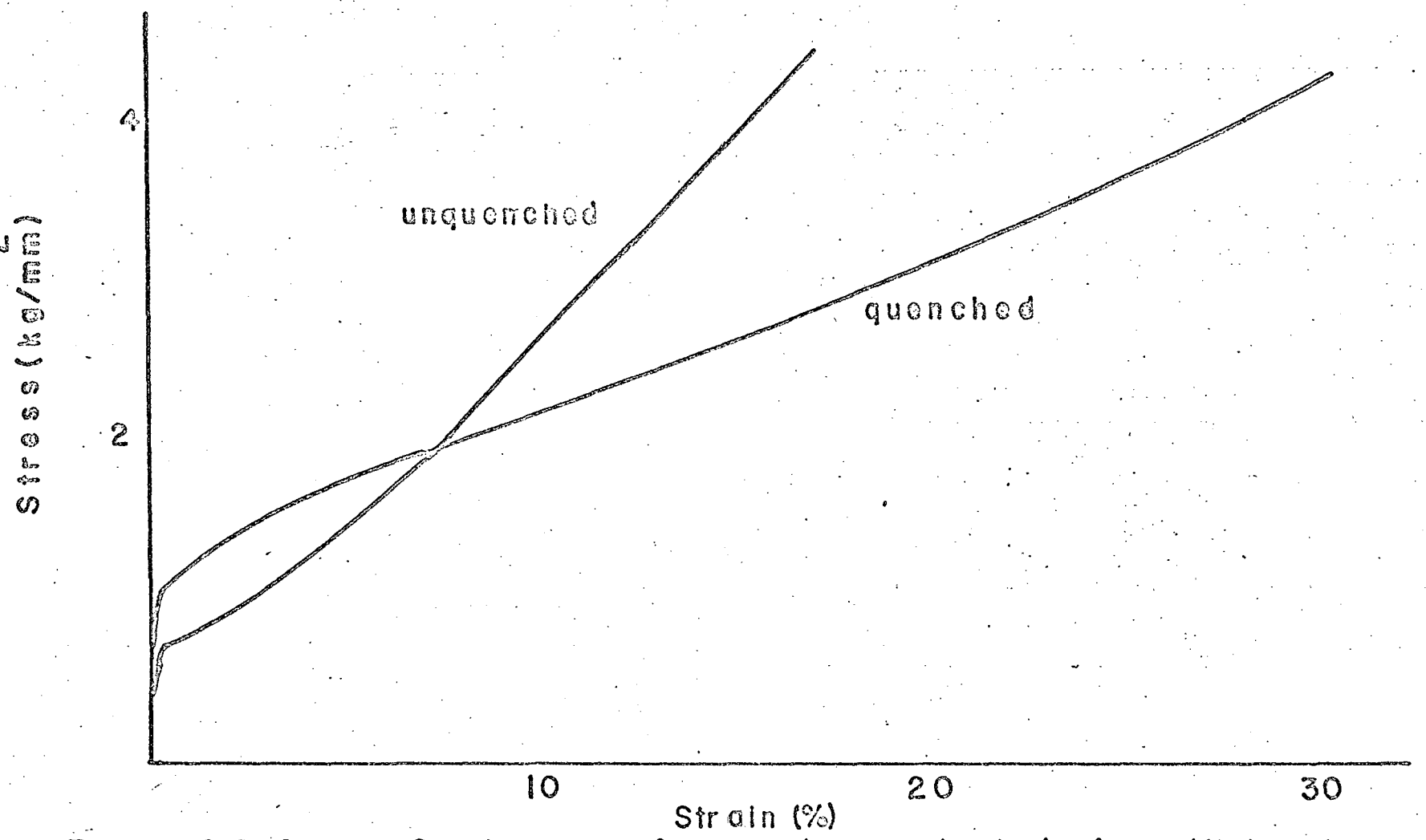

Figure 29 Stress-Strain curve for specimen oriented for multiple slip. Specimen aged 17 hours at room temperature.

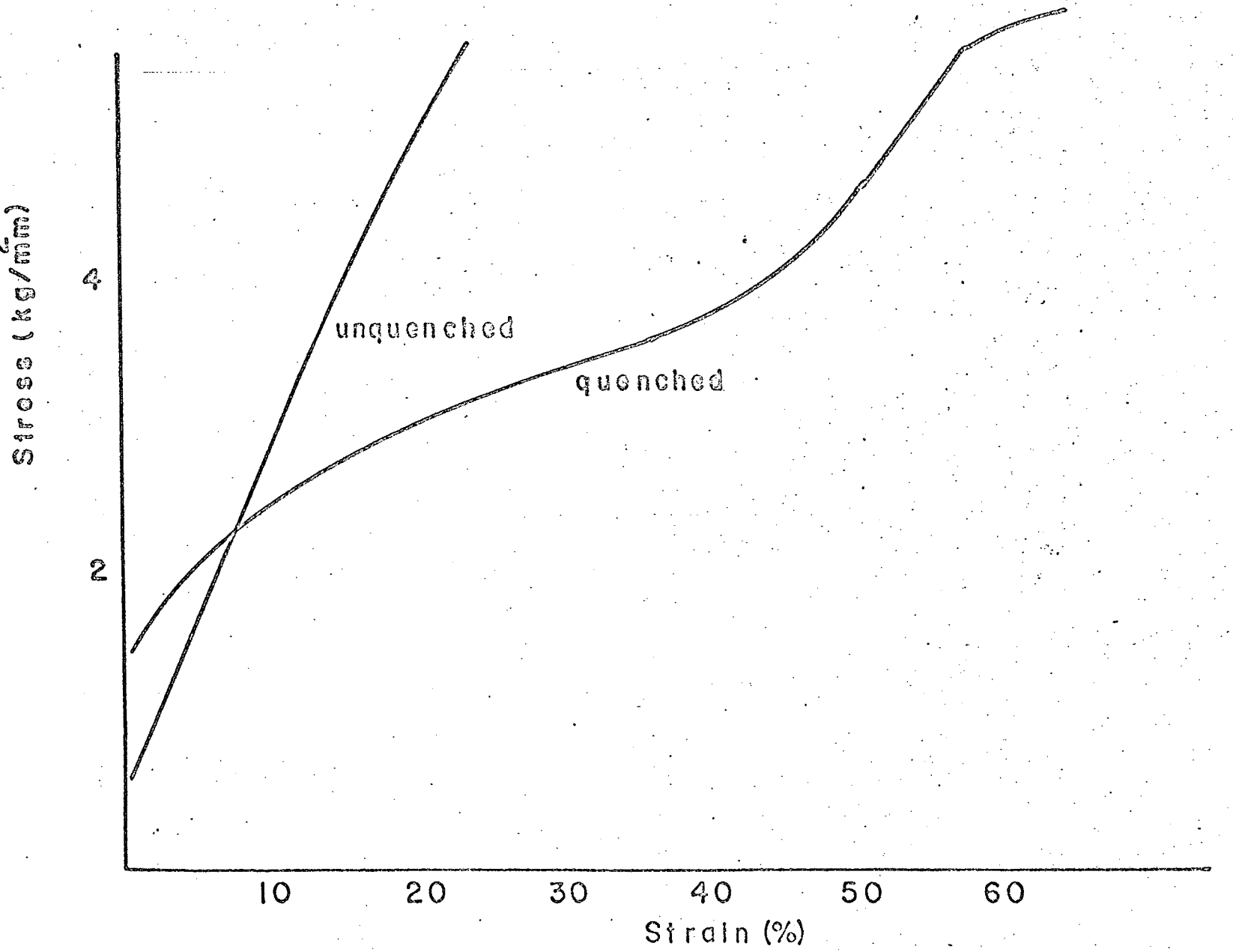

Figure 3.0 Stress-Strain curve for multiple slip specimen aged 5 days at 25° C

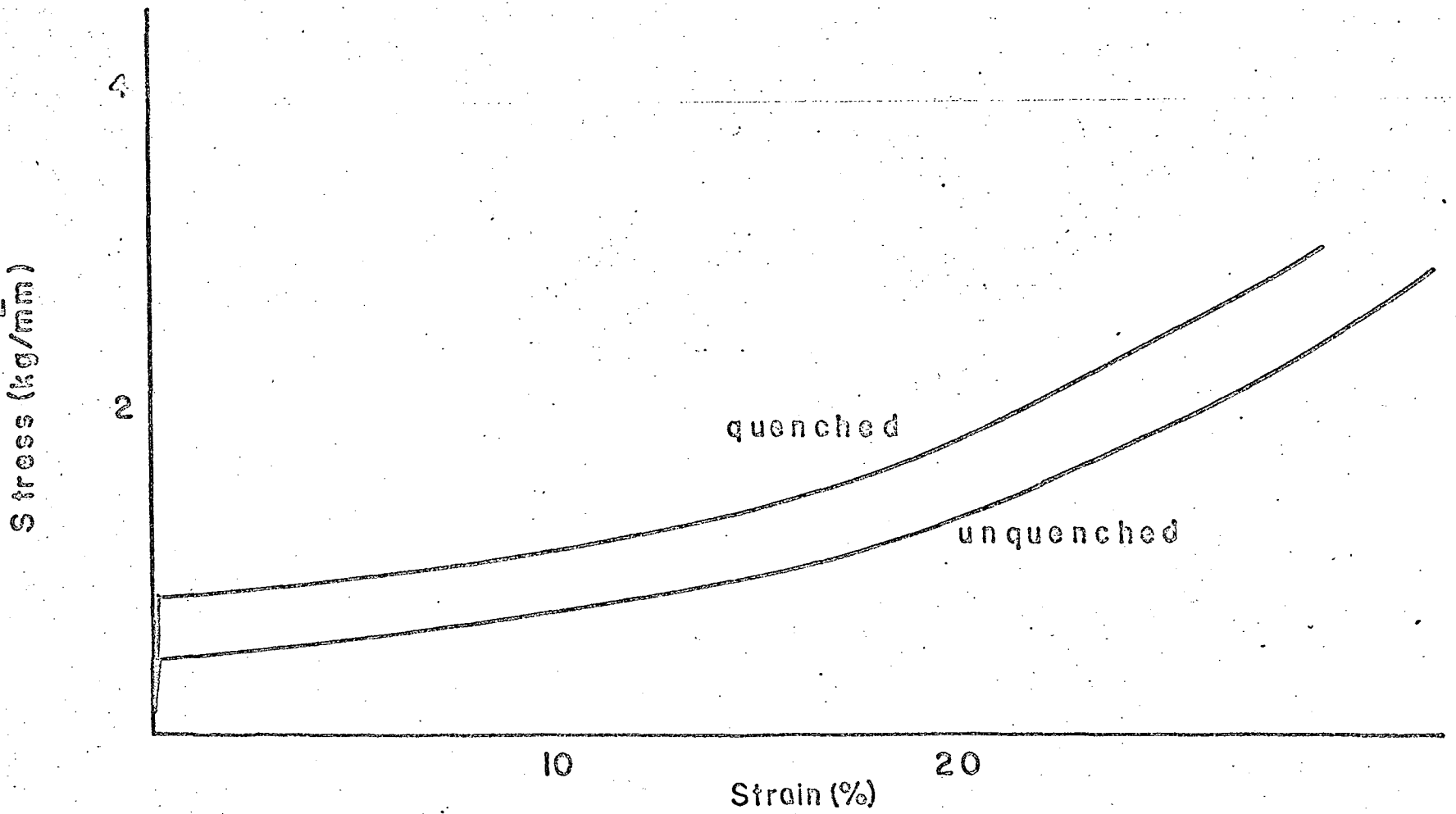

Figure 31 Stress - Strain curve for specimen aged 10 minutes at room temperature, and deformed at 4.2 °k.

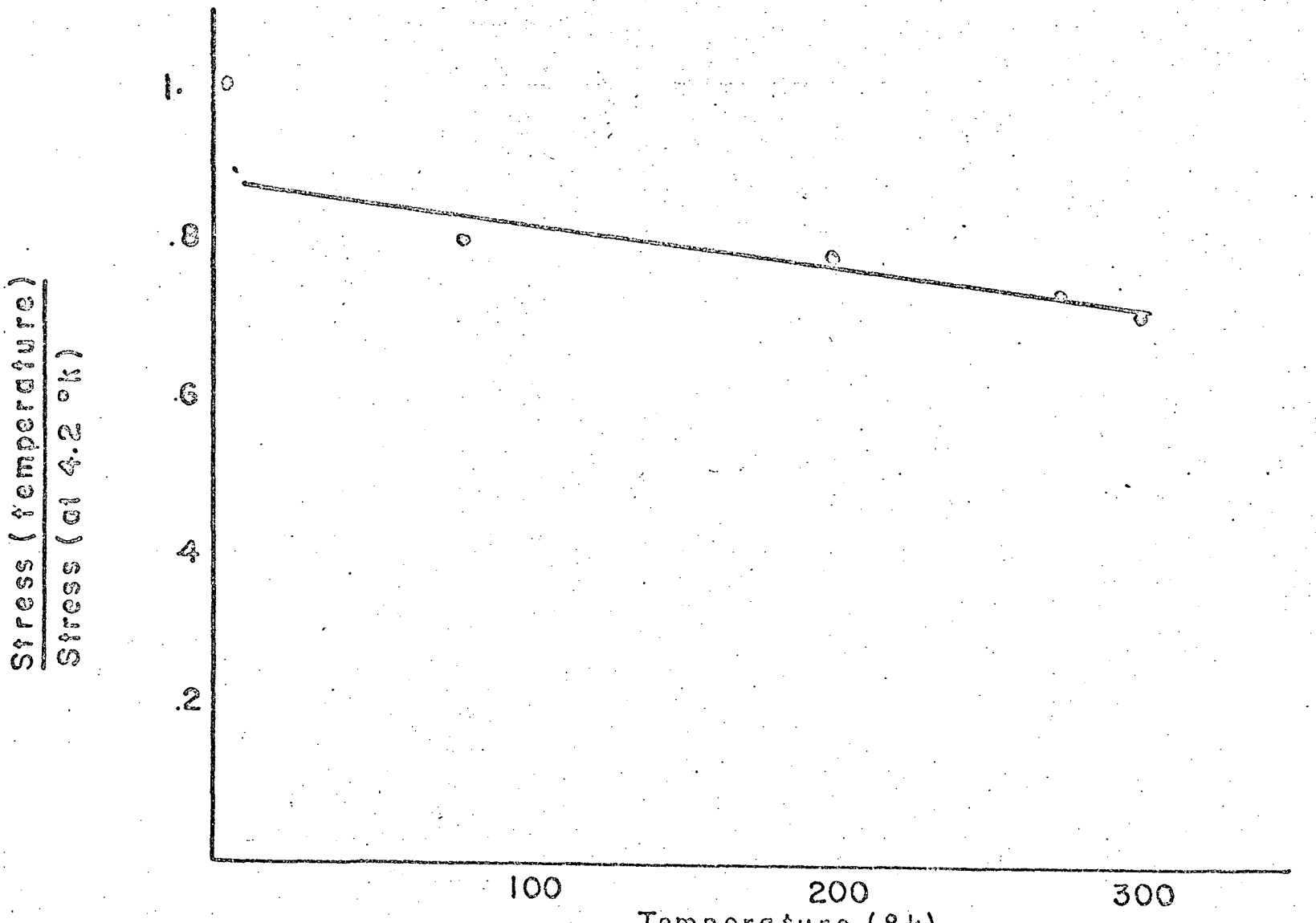

Figure 32 Temperature dependence of the yield stress for a specimen aged 10 minutes at room temperature

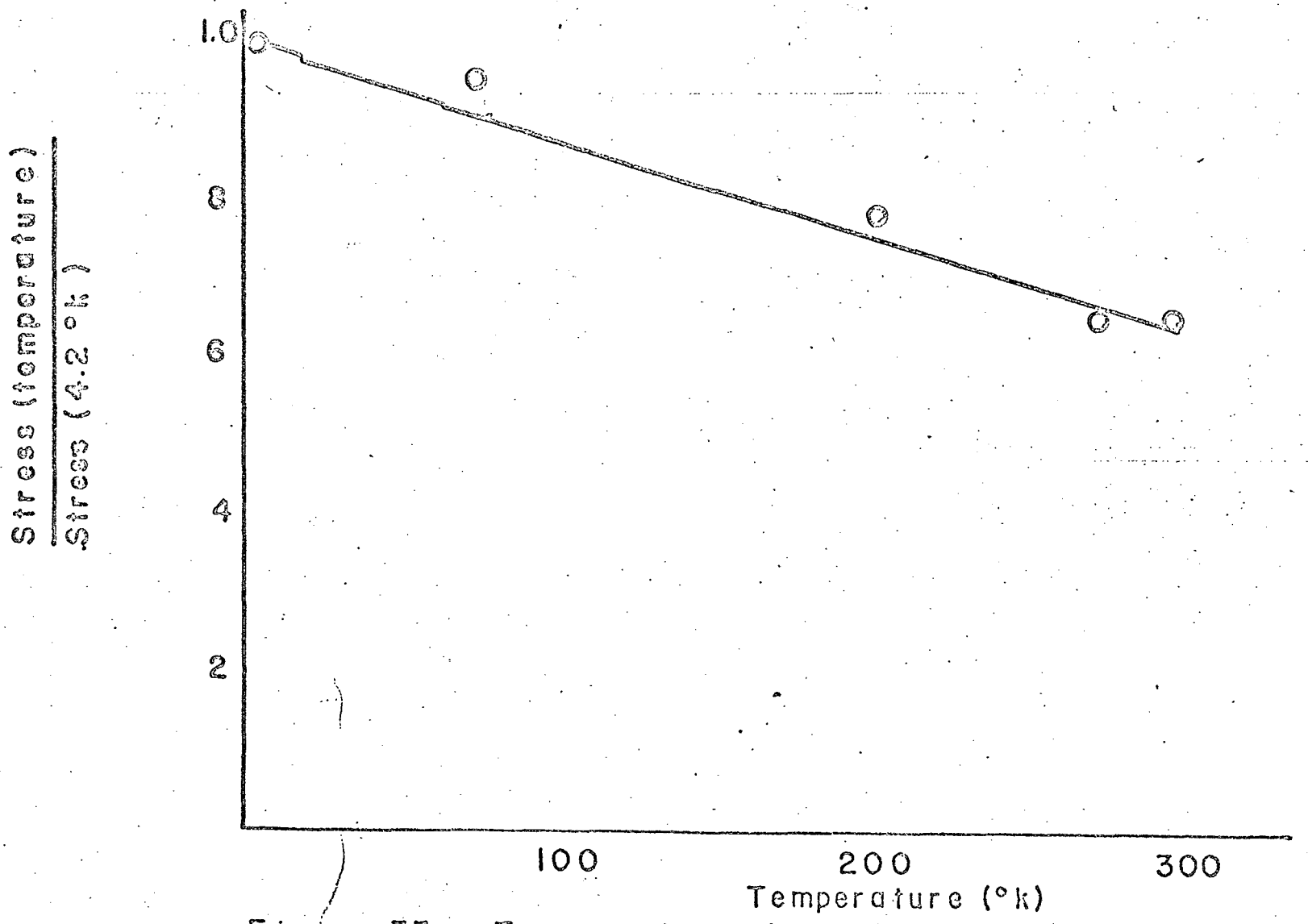

Figure 33 Temperature dependence of the yield stress for a specimen aged 10 hours at room temperature